



HAL
open science

Chromium hazard and risk assessment: New insights from a detailed speciation study in a standard test medium.

Imad Aharchaou, Jean-Sébastien Py, Sébastien Cambier, Jean-Luc Loizeau, Geert Cornelis, Philippe Rousselle, Eric Battaglia, Davide Anselmo Luigi Vignati

► To cite this version:

Imad Aharchaou, Jean-Sébastien Py, Sébastien Cambier, Jean-Luc Loizeau, Geert Cornelis, et al.. Chromium hazard and risk assessment: New insights from a detailed speciation study in a standard test medium.. *Environmental Toxicology and Chemistry*, 2017, 37 (4), pp.983 - 992. 10.1002/etc.4044 . hal-01906558

HAL Id: hal-01906558

<https://hal.science/hal-01906558>

Submitted on 26 Oct 2018

HAL is a multi-disciplinary open access archive for the deposit and dissemination of scientific research documents, whether they are published or not. The documents may come from teaching and research institutions in France or abroad, or from public or private research centers.

L'archive ouverte pluridisciplinaire **HAL**, est destinée au dépôt et à la diffusion de documents scientifiques de niveau recherche, publiés ou non, émanant des établissements d'enseignement et de recherche français ou étrangers, des laboratoires publics ou privés.

1 This is the accepted version of the following article:

2
3
4
5
6
7
8
9
10
11
12
13
14
15
16
17
18
19
20
21
22
23
24
25
26
27
28
29
30
31
32
33
34
35
36
37
38
39
40
41
42
43
44
45
46
47
48
49
50

Aharchaou I, Py J-S, Cambier S, Loizeau J-L, Cornelis G, Rousselle P, Battaglia E, Vignati DAL. Chromium hazard and risk assessment: New insights from a detailed speciation study in a standard test medium. Environmental Toxicology and Chemistry, DOI: 10.1002/etc.4044

which has been published in final form at
<http://onlinelibrary.wiley.com/wol1/doi/10.1002/etc.4044/abstract>.

This article may be used for non-commercial purposes in accordance with the Wiley Self-Archiving Policy <https://authorservices.wiley.com/author-resources/Journal-Authors/licensing-open-access/open-access/self-archiving.html>.

51 **CHROMIUM HAZARD AND RISK ASSESSMENT: NEW INSIGHTS FROM A**
52 **DETAILED SPECIATION STUDY IN A STANDARD TEST MEDIUM**

53
54 Imad Aharchaou^a, Jean-Sébastien Py^b, Sébastien Cambier^c, Jean-Luc Loizeau^d, Geert Cornelis^e,
55 Philippe Rousselle^a, Eric Battaglia^a, Davide A.L. Vignati^{a*}
56

57 ^aLaboratoire Interdisciplinaire des Environnements Continentaux UMR 7360, Université de Lorraine
58 and CNRS, Metz, France

59 ^bAgence nationale de sécurité sanitaire de l'alimentation, de l'environnement et du travail, Laboratoire
60 de Nancy, Nancy, France

61 ^cLuxembourg Institute of Science and Technology, Esch sur Alzette, Luxembourg

62 ^dDepartment F.-A. Forel for Environmental and Aquatic Sciences and Institute for Environmental
63 Sciences, University of Geneva, Genève, Switzerland

64 ^eSwedish University of Agricultural Sciences, Department of Soil and Environment, Uppsala, Sweden
65
66
67
68
69
70
71
72

73 **ABSTRACT**

74 Despite the consensus about the importance of chemical speciation in controlling the
75 bioavailability and ecotoxicity of trace elements, detailed speciation studies during laboratory
76 ecotoxicity testing remain scarce, contributing to uncertainty when extrapolating laboratory
77 findings to real field situations in risk assessment. We characterized the speciation and
78 ecotoxicological effects of Cr^{III} and Cr^{VI} in the OECD medium for algal ecotoxicity testing.
79 Total and dissolved (< 0.22 μm) Cr concentrations showed little variability in media spiked
80 with Cr^{VI}, while dissolved Cr concentration decreased by as much as 80% over 72 hours in
81 medium amended with Cr^{III}. Analyses by ion chromatography ICP-MS highlighted the
82 absence of redox interconversion between Cr^{III} or Cr^{VI} both in the presence and absence of
83 algal cells (*Raphidocelis subcapitata*). Furthermore, the concentration of ionic Cr^{III} dropped
84 below detection limits in less than 2 hours with the corresponding formation of carbonate
85 complexes and Cr hydroxides. Precipitation of Cr^{III} in the form of colloidal particles of
86 variable diameters was confirmed by nanoparticle tracking analysis, spICP-MS and single
87 particle counting. In terms of time weighted dissolved (< 0.22 μm) Cr concentration, Cr^{III} was
88 4 to 10 times more toxic than Cr^{VI}. However, Cr^{III} ecotoxicity could arise from interactions
89 between free ionic Cr^{III} and algae at the beginning of the test, from the presence of Cr-bearing
90 nanoparticles or a combination of the two. Future ecotoxicological studies must pay more
91 attention to Cr speciation to reliably compare the ecotoxicity of Cr^{III} and Cr^{VI}.
92

93 **Keywords**

94 Trace metals, Chromium, Metal speciation, Algae, Hazard/Risk assessment
95
96
97
98
99
100
101

102 INTRODUCTION

103 The bioavailability and ecotoxicity of trace elements in natural environments are determined
104 by the complex interplay among the ecological traits of living organisms, the toxicodynamics
105 and toxicokinetics of trace elements, and the elemental speciation in environmental matrices
106 (Fairbrother et al. 2007; Mason 2013; Harris et al. 2014). Elemental speciation refers to
107 various physico-chemical forms in which trace elements occur in a given environment and, in
108 some cases, includes the presence of different oxidation states with contrasting environmental
109 biogeochemistry. In the specific case of chromium, the importance of speciation is well
110 appreciated with regard to its biogeochemical cycle (Masscheleyn et al. 1992; Dominik et al.
111 2007; Saputro et al. 2014) and biological effects (WHO 2009; WHO 2013). In surface waters,
112 chromium mainly occurs in two oxidation states, namely Cr^{VI} and Cr^{III}, with contrasting
113 environmental and biological behavior. Hexavalent chromium, a recognized human
114 carcinogen, forms negatively charged chemical species, interacts little with colloidal and
115 particulate material, has a high environmental mobility, and easily crosses biological
116 membranes (WHO 2013). In contrast, Cr^{III} preferentially forms positively charged chemical
117 species, tends to associate with colloids or suspended particulate matter and is considered of
118 less ecotoxicological concern (WHO 2009; WHO 2013). In most environmental settings, both
119 redox forms occur simultaneously, albeit in variable proportions (Bobrowski et al. 2004;
120 Saputro et al. 2014) and interconversions between them have been documented along with the
121 corresponding controlling factors (Rai et al. 1989; Richard and Bourg 1991; Lin 2002).
122 However, experimental research on Cr speciation in standardized ecotoxicological test media
123 has received limited attention. Thermodynamic speciation calculations are increasingly used
124 to predict the Cr forms likely to exist in ecotoxicological exposure media, thus aiding
125 experimental planning and data interpretation (Dazy et al. 2008; Didur et al. 2013; Liu et al.
126 2015). These calculations also suggest that insoluble species of Cr^{III} (mostly Cr oxy-
127 hydroxides) can form in ecotoxicological test media for algae, daphnids and aquatic plants
128 (Dazy et al. 2008; Vignati et al. 2010; Ponti et al. 2014). The presence of such chemical
129 species can modify the fraction of Cr^{III} that is potentially bioavailable for the test organisms
130 during the exposure period, because in most cases it is assumed that the bio-availability of
131 metals is related to the free ion activity (Morel, 1983). Insoluble species also explain the often
132 large differences between total and total filterable (< 0.45 µm) Cr concentrations found in test
133 media spiked with Cr^{III}, the extent depending on medium composition (Chapman et al. 1980;
134 Vignati et al. 2008; Ponti et al. 2014). It should also be noted that filterable (< 0.45 µm) Cr
135 concentrations do not equal the sum of concentrations of truly dissolved Cr species, because
136 the initial formation of precipitates may result in solids having particle sizes below this size
137 cut-off. Furthermore, certain studies present results supporting the conclusion that Cr^{III} is
138 more ecotoxic than Cr^{VI} (Holdway 1988; Thompson et al. 2002; Vignati et al. 2010; Lira-
139 Silva et al. 2011; Kováčik et al. 2015); in contrast with the current consensus considering Cr^{VI}
140 as the most ecotoxic redox form (WHO 2013). A more detailed understanding of Cr
141 speciation in (standardized) laboratory test media used for ecotoxicity testing will help to both
142 reconcile contrasting ecotoxicological results in controlled settings and improve our ability to
143 extrapolate laboratory results to real-field risk assessment situations.

144 On the basis of the above considerations, three aspects related to Cr speciation, and its
145 changes during a given (standardized) test, appear of particular importance for an improved
146 understanding of the relative ecotoxicity of Cr^{III} and Cr^{VI}: a) the stability of (filterable) Cr
147 concentrations added to the test medium, b) the possibility of redox interconversions between
148 Cr^{III} and Cr^{VI}, and c) the formation of Cr oxyhydroxides (i.e., Cr-bearing nanoparticles). In
149 the present study, the ecotoxicity of three Cr^{III} salts and one Cr^{VI} salt commonly used in
150 ecotoxicological studies was investigated using the standard algal medium ISO 8692 (OECD
151 2011), hereinafter test medium, as exposure matrix and the green alga *Raphidocelis*

152 *subcapitata* as test organism. The behavior and speciation of both Cr^{III} and Cr^{VI} forms,
153 including their possible interconversions, were investigated in detail over 72 h; corresponding
154 to the typical duration of a standard algal test (OECD 2011). Our results showed rapid
155 changes (i.e., within hours) in Cr^{III} speciation which calls for a thorough reconsideration of
156 the current knowledge about the relative ecotoxicity of Cr^{III} and Cr^{VI} in terms of both hazard
157 and risk assessment.

158

159 **MATERIALS AND METHODS**

160 *Chemicals*

161 All chemicals used were of highest purity. For the various experiments, the test medium
162 ISO8692 was prepared as described in OECD guideline 201 (OECD 2011) and spiked with
163 either Cr^{VI} as potassium dichromate (K₂Cr₂O₇, VWR, purity 99.8% min, CAS number 7778-
164 50-9) or with one of the following Cr^{III} salts: chromium chloride (CrCl₃·6H₂O; Alfa Aesar,
165 99.5% min, Crystalline, CAS number 10060-12-5), chromium potassium sulfate
166 (KCr(SO₄)₂·12H₂O; VWR, 99%, CAS number 7788-99-0) or chromium nitrate
167 (Cr(NO₃)₃·9H₂O; Alfa Aesar, 98.5%, Crystalline, CAS number 7789-02-8).

168 All filtrations were performed using 0.22 µm syringe filters (Millex 33 mm diameter, PVDF,
169 Millipore, reference number SLGV033NB) prewashed one time with 10 mL of diluted (10%
170 v/v) hydrochloric acid (HCl Suprapur 30%, Merck Millipore, lot number Z0309518344) and
171 three times with 10 mL of ultrapure water (Millipore, Q-POD®). A preliminary experiment
172 showed that Millex syringe filters with nominal pore sizes of 0.22 and 0.45 µm yielded
173 comparable results for aliquots of test medium amended with 60 µg Cr^{III}/L (data not shown).
174 All samples for the analysis of total Cr concentration were acidified at 1% v/v with
175 concentrated nitric acid (HNO₃ 67%, Prolabo, VWR, batch number 1108110). A solution of
176 0.4 M nitric acid (Chemlab, suprapur 70%, batch: 221831609) spiked with 1 µg/L of rhodium
177 was used as internal standard during the analyses of Cr speciation.

178

179 *Chromium ecotoxicity*

180 The ecotoxicity of Cr^{VI} and Cr^{III} salts to the green alga *Raphidocelis subcapitata* (strain 278/4
181 originally obtained from the Culture Collection of Algae and Protozoa – CCAP – Argyll,
182 Scotland, United Kingdom; formerly known as *Pseudokirchneriella subcapitata*) was
183 evaluated according to OECD guideline 201 (OECD 2011). Tests were performed as
184 previously described (Vignati et al. 2010) using inoculums of 20,000 cells/mL and nominal
185 exposure concentrations of 9, 18, 35, 70, 140, 280, 560, 1125, 2250 µg Cr/L. The effects of Cr
186 salts on algal growth were expressed as the effective exposure concentrations (ECs₅₀) that
187 produced a 50% decrease in algal fluorescence (BMG LabTechnologies, Fluostar), considered
188 as a proxy for algal biomass. The ECs₅₀ were calculated by performing a nonlinear regression
189 on Hill's model with the macro REGTOX (Version EV7.0.4., E. Vindimian) (Vindimian
190 2010). In the case of Cr^{III}, ECs₅₀ were estimated based on both nominal concentrations and
191 Time-Weighted Mean (TWM) dissolved measured concentrations (OECD 2012). Starting
192 from this point, the terms total and dissolved concentrations will indicate the unfiltered and
193 filtered (0.22 µm) portions of measured Cr levels.

194

195 *Temporal evolution of Cr concentration in the test medium*

196 Aliquots (50 mL) of freshly prepared test medium were transferred to acid-washed
197 Erlenmeyer flasks (150 mL) and spiked with a Cr concentration corresponding to the ECs₅₀
198 of either Cr^{III} (added as CrCl₃·6H₂O) or Cr^{VI} (added as K₂Cr₂O₇) in the presence or absence of
199 an initial algal inoculum of 20,000 cells/mL. Aliquots were analyzed for total and dissolved
200 Cr after 0.5, 1, 2, 4, 8, 24, 48, and 72 h of incubation under continuous light (90 – 110
201 µE/m²/s) at 21 ± 2 °C and, for biotic samples only, rotary agitation (100 rpm). For dissolved

202 Cr determination, the first 5 mL of filtered solution were used for preconditioning the filters
203 and discarded. Preconditioning aimed at removing possible residues of ultrapure water from
204 filter pores and saturate possible sorption sites for Cr. Total and dissolved Cr concentrations
205 were determined by flame atomic absorption spectrometry (FAAS, Perkin-Elmer AAnalyst
206 100) or, for concentrations < 20 µg/L, graphite furnace atomic absorption spectrometry
207 (GFAAS, Varian spectra 300, using 0.1% Mg(NO₃)₂ as matrix modifier according to
208 manufacturer instructions). Quantification limits were 10 µg/L for FAAS and 0.2 µg/L for
209 GFAAS. Certified reference materials SPS-SW1 (2.00 ± 0.02 µg/L) and WW1 (200 ± 1
210 µg/L), both from SpectraPure standards (Manglerud, Norway), were used as quality controls.
211 All analytical results are expressed in µg Cr/L.

212 The statistical significance of the temporal changes in Cr concentrations was evaluated by
213 one-way ANOVA with Tukey post-hoc comparison. Visual Minteq modelling (ver 3.1) was
214 done to investigate Cr^{III} speciation in test medium amended with an initial total concentration
215 of 60 µg Cr/L. No redox transformations were assumed, because it will be argued based on
216 experimental proof that these did not occur. Calculations were performed using
217 experimentally measured Cr concentrations and pH values, and the test medium composition
218 as reported in OECD (2011). No modifications were made to the Visual Minteq default
219 database and the Debye-Hückel equation was used for activity corrections.

220 221 *Chromium redox speciation*

222 To investigate Cr redox speciation and the possible interconversion between Cr^{III} and Cr^{VI},
223 aliquots (50 mL) of the test medium were spiked with either Cr^{VI} or Cr^{III} (added as chloride)
224 both in absence (abiotic medium) and presence (biotic medium) of algal inoculums (20,000
225 cells/mL). Nominal Cr concentrations in the spiked solutions were 60 µg/L for Cr^{III} and 115
226 µg/L for Cr^{VI}, corresponding to the calculated 72 h ECs₅₀ (see section Chromium ecotoxicity
227 in Results and discussion). Samples were analyzed immediately after spiking (t=0) or
228 incubated at 23 ± 1 °C, under continuous light (90 – 110 µE/m²/s) and, for biotic samples
229 only, rotary agitation (100 rpm) for 24, 48 and 72 h prior to analysis (Figure S1). At the end
230 of each incubation period, sample aliquots for Cr speciation were filtered as described above.
231 After preconditioning the filters with 5 mL (subsequently discarded) of Cr-amended test
232 medium, 10 mL of filtrate was collected in polystyrene sample vials and immediately
233 analyzed by ion chromatography-inductively coupled plasma mass spectrometry (IC-ICP-
234 MS). Samples were kept at between 4 and 6 °C in a refrigerated sample tray during analysis.
235 An additional abiotic sample of test medium (2 L) was prepared in an acid-washed low-
236 density polyethylene bottle and spiked with 60 µg/L of Cr^{III} to follow more closely the
237 kinetics of the changes in Cr^{III} speciation (Sacher et al. 1999; Séby et al. 2003). Aliquots for
238 analysis were recovered every 20 min over the first 6 hours after spiking and again after 24,
239 48, and 72 hours of incubation in the same conditions described above.

240 Trivalent Cr and hexavalent Cr species were separated and quantified by IC-ICP-MS using a
241 Thermo ICS 5000+ pump coupled with an anion exchange column (Thermo AG7 2x50 mm)
242 and connected to the nebulizer of an ICP-MS (Thermo, Series XII) (Table S1). A solution of
243 0.4 M nitric acid spiked with 1 µg/L of rhodium was used to elute the Cr species from the
244 anion exchange column (see Table S1 for more details). The analyses were carried out
245 according to the method developed by the French Agency for Food, Environmental &
246 Occupational Health & Safety (ANSES) on the basis of the application note from the supplier
247 (Sacher et al. 1999; ANSES/LHN/MT-CrVI). Chromium detection was performed at m/z 52
248 and 53. Experimental IC-ICP-MS results were compared with those of speciation modeling
249 carried out as described previously (section Temporal evolution of Cr concentration) using
250 Visual Minteq.

251

252 *Formation of Cr nanoparticles in the test medium*

253 Aliquots of test medium were spiked with 60 µg/L of Cr^{III} (added as chloride or nitrate) and
254 the formation of Cr-containing particles was investigated by Nanoparticle Tracking Analysis
255 (NTA), spICP-MS (single particle ICP-MS) and Single Particle Counting (SPC) over 72 h;
256 that is the typical duration of an algal ecotoxicological test. Blank samples consisting of
257 unspiked test medium were systematically analyzed along with the corresponding samples.
258 Total and dissolved Cr concentrations were determined by FAAS during the various
259 experiments.

260 For NTA (Nanosight NS500; Malvern instruments Ltd, UK), spiked samples were aged for 0,
261 0.5, 1, 2, 24, 48, and 72 h and assayed (before and after filtration) for particle concentration
262 and particle size distribution (PSD). The NS500 provides detailed analysis of the
263 concentration and size distribution of all types of nanoparticles from 10 nm to 1000 nm in
264 diameter (Carr and Wright 2013) using the properties of both light scattering and Brownian
265 motion in liquid suspensions. Particles in suspension in the sample chamber (volume = 0.3
266 mL) were visualized using a 20x magnification microscope equipped with a camera operated
267 at 25 frames per second for 60 s. The resulting video files were elaborated using the built-in
268 software (NTA 2.3 build 0033) to calculate the hydrodynamic diameter of the individually
269 tracked particles. After each measurement, the sample chamber was flushed with milliQ water
270 and reloaded with the next sample aliquot. All measurements were done in triplicate and the
271 mean (\pm one standard deviation) of particle concentration and average size calculated (see
272 supplementary information for protocol optimization).

273 While NTA determines the total particle count, spICP-MS (Perkin Elmer NexION 350D ICP-
274 MS) was used to specifically measure Cr-containing particles. Samples were aged for 0, 24,
275 48 and 72 h and diluted to a theoretical concentration of 0.06 µg/L total Cr before analysis.
276 The transport efficiency was calculated based on a dissolved standard curve of Au stabilized
277 by 0.1 % cysteine and on the TEM-based median size (56 nm) of gold nanoparticles
278 (NIST8013, nominal diameter 60 nm) using the method of Pace et al. (2011). Data acquisition
279 was performed in fast acquisition scanning technique (FAST) mode with a dwell time of 50
280 µs over 100 s. Raw data (two million readings per sample) were extracted and loaded into the
281 Nanocount software (<http://blogg.slu.se/nanocount/>) for the determination of particle number
282 and particle size distribution. Correction for dissolved concentrations was performed using
283 outlier analysis based on a $5 \times \sigma$ criterion specifically developed for FAST data (Tuoriniemi
284 et al. 2015). Peak integration time was set to 20 ms and the minimum detectable cluster was
285 set at 4 ions. Distributions of the corresponding spherical size were calculated assuming a
286 Cr(OH)₃ ($\rho = 3.11 \text{ g/cm}^3$) composition and a spherical shape. It should be noted that these
287 were assumptions as the exact composition and shape of the formed particles are unknown.

288 However, considering the measured pH range of the test medium initially spiked with 60 µg
289 Cr/L (7.8–7.9 units), trivalent chromium is expected to rapidly undergo hydrolysis and form
290 amorphous oxyhydroxides (Rai et al. 1989; Kotaš and Stasicka 2000). The assumption on
291 particle shape would allow comparison with the results obtained using other methods.
292 To detect the presence of particles outside the NTA and spICP-MS measuring range, samples
293 were analyzed after 0, 24, 48, and 72 hours of incubation using three Single Particle Counters
294 (SPCs): a high sensitivity in-situ monitor (HSLIS) Model M50 for the range 50 to 200 nm and
295 two Volumetric Spectrometers (LiQuilaz-S02 and LiQuilaz-S05, Particle Measuring Systems,
296 Boulder, CO, U.S.A) for the ranges 200 to 2000 nm and 500 nm to 20 µm, respectively. The
297 SPCs use light scattering to count individual particles across 31 size classes with some
298 overlapping between the LiQuilaz-S02 and S05 (Rossé and Loizeau 2003). Results for spiked
299 medium were corrected for blank values.

300

301

302 RESULTS AND DISCUSSION

303 *Chromium ecotoxicity and temporal evolution of Cr concentrations*

304 Results of ecotoxicity tests were highly reproducible with ECs50 at 72 h (mean value \pm one
305 standard deviation) of 113 ± 3 $\mu\text{g/L}$ ($n = 3$) for $\text{K}_2\text{Cr}_2\text{O}_7$, 59 ± 3 $\mu\text{g/L}$ for $\text{CrCl}_3 \cdot 6\text{H}_2\text{O}$ ($n = 6$),
306 61 ± 8 $\mu\text{g/L}$ for $\text{Cr}(\text{NO}_3)_3 \cdot 9\text{H}_2\text{O}$ ($n = 3$) and 62 ± 3 $\mu\text{g/L}$ for $\text{KCr}(\text{SO}_4)_2 \cdot 12\text{H}_2\text{O}$ ($n=3$). The
307 ECs50 values reported in the literature for freshwater algae range from 130 to 470 $\mu\text{g/L}$ for
308 Cr^{VI} and from 30 $\mu\text{g/L}$ to over 1000 $\mu\text{g/L}$ for Cr^{III} (WHO 2009; Vignati et al. 2010; OECD
309 2011; WHO 2013). In the case of Cr^{VI} , a ring test involving 16 laboratories determined a
310 range of 72h-ECs50 between 70 and 260 $\mu\text{g Cr/L}$ for *Scenedesmus subspicatus* and
311 *Selenastrum capricornutum* (a former name for *R. subcapitata*) based on algal biomass
312 endpoint (Munn et al. 2005; WHO 2013); which agrees with our results. In the case of Cr^{III} ,
313 our results are in the low range of the values reported in the literature and indicate a higher
314 toxicity of Cr^{III} compared with Cr^{VI} ; an occurrence also reported in previous research
315 (Holdway 1988; Thompson et al. 2002; Vignati et al. 2010; Lira-Silva et al. 2011; Kováčik et
316 al. 2015). Further insights in the relative ecotoxicity of the two redox forms of Cr can be
317 gained by examining their behavior in the test medium. In particular, the detailed examination
318 of Cr^{VI} and Cr^{III} behavior added to the test medium at concentrations corresponding to their
319 respective ECs50 allows to exactly determine the actual concentrations responsible for the
320 observed effects.

321 At $t = 0$ h, the measured total and dissolved Cr concentrations (added as Cr^{III}) were similar
322 and corresponded to the expected nominal values in both abiotic and biotic media. In the
323 absence of algae, total Cr concentrations remained within 20% of the initial value over the
324 first 24 hours and had decreased by about 40% after 72 h. In the same experiment, dissolved
325 Cr concentrations remained within 20% of the initial values only over the first two hours, but
326 had dropped by 40% eight hours after spiking and by 83% after 72 h (Figure 1). The decrease
327 in total Cr concentrations indicates that some of the added Cr may be lost to the walls of the
328 test vessel over time. However, comparison of total and dissolved concentrations indicates
329 that ca. 50% of the added Cr likely occurs in the form of colloidal or particulate form (most
330 likely amorphous Cr oxyhydroxides) starting from 24 hours after spiking (i.e., for over 2/3 of
331 the test duration). Calculations in Visual Minteq for an initial concentration of 60 $\mu\text{g/L}$ as Cr^{III}
332 predicted that, in the observed pH range of 7.8 to 7.9, the $\text{Cr}(\text{OH})_3$ species should account for
333 92–94 % of the total Cr. Furthermore, about 80% of the initially added Cr^{III} was predicted to
334 precipitate in the form of amorphous $\text{Cr}(\text{OH})_3$, in very good agreement with the 80% decrease
335 of the corresponding dissolved Cr concentration over 72h (Figure 1). Colloid/nanoparticle
336 formation was indeed confirmed using NTA and spICP-MS (see section Formation of Cr
337 nanoparticles in Results and Discussion). Analogous calculations using the dissolved Cr
338 concentration measured at 72h (11 ± 0.25 $\mu\text{g/Cr L}$, $n=3$) also predicted that $\text{Cr}(\text{OH})_3$ would
339 account for over 90% of the measured Cr concentration, but with less than 2% occurring in
340 the precipitated phase. In both cases, the sum of the positively charged species $\text{Cr}(\text{OH})_2^+$ and
341 CrOH^{2+} was predicted to represent about 3.5% of the total dissolved Cr and EDTA complexes
342 were about 2.5%. Further comparison between speciation calculations and analytical results is
343 presented in the next section.

344 The difference between total and dissolved Cr concentrations becomes statistically significant
345 starting from 8 h after spiking (one-way Anova with Tukey post-hoc comparison, $p < 0.01$).
346 Considering the temporal decrease of the dissolved Cr concentration, assumed as a better
347 proxy of the Cr potentially available to the algae (see de Paiva Magalhães et al. 2015 and
348 references therein for a detailed discussion), the time-weighted mean (TMW) (OECD 2012)
349 exposure concentration of the algae to Cr (added as Cr^{III}) was about 25 $\mu\text{g/L}$ for an initial
350 addition of 60 $\mu\text{g/L}$ as Cr^{III} . Similar behavior of total and dissolved Cr concentration was
351 observed over the concentration range 20 – 7,000 $\mu\text{g/L}$ for CrCl_3 and for selected

352 concentrations of $\text{Cr}(\text{NO}_3)_3$ and CrKSO_4 (Figures S2–S4); confirming that the decrease in the
353 dissolved exposure concentrations must be considered and quantified when testing Cr^{III}
354 toxicity in standardized laboratory media. These observations corroborate previous findings
355 obtained by measuring the decrease in Cr concentrations in test medium directly in 96-well
356 microplates in the absence of algae and without actually providing information on the total vs.
357 dissolved Cr concentrations (Vignati et al. 2008; Vignati et al. 2010).
358 In the presence of algae, both total and dissolved Cr concentrations decreased with time
359 (Figure 1) and the decrease was more marked for the dissolved concentrations (over 95% after
360 72 hours). The incomplete recovery of total Cr was likely caused by attachment of algal cells
361 to the vessel's walls despite the constant agitation. Most importantly, the differences between
362 dissolved Cr concentrations in the absence and presence of algae became statistically
363 significant starting from 24 h after spiking (one-way Anova with Tukey post-hoc comparison,
364 $p < 0.01$), indicating adsorption onto or absorption into the algal cells of most of the available
365 dissolved Cr. Based on the dissolved Cr concentrations in the presence of algae, the 72 h
366 TMW effect concentration (EC50) for algal growth (in terms of biomass) was $11.5 \mu\text{g/L}$.
367 Analogous experiments performed with aliquots of test medium amended with Cr^{VI} at the
368 corresponding EC50 concentration ($115 \mu\text{g/L}$) did not show significant changes in total or
369 dissolved Cr concentration neither in the absence nor in the presence of algae (Figure S5).
370 The above observations lead us to the conclusion that Cr^{III} is 4 to 10 times more toxic than
371 Cr^{VI} when the 72 h EC50 for Cr^{III} is expressed as the TWM dissolved concentration estimated
372 from measurements in the absence or presence of algae, respectively. However, the presence
373 of algae had no measurable effect on dissolved Cr^{VI} concentrations (Figure S6). One
374 possibility is that the entrance of minimal quantities of Cr^{VI} into the cells may suffice to
375 reduce algal biomass, which would support the current consensus that Cr^{VI} is more toxic than
376 Cr^{III} . On the other hand, exposure to Cr^{VI} has been shown to cause lysis of *R. subcapitata*
377 cells at concentrations of 1.75 mg/L or higher added to an algal inoculum of $2 \times 10^5 \text{ cells/mL}$
378 (Labra et al. 2007); which corresponds to an initial quantity of 8.75 ng of Cr^{VI} per algal cell at
379 the beginning of the experiment (our calculation). This figure compares favorably with the
380 value of 5.75 ng of Cr^{VI} per algal cell in our experimental conditions for an initial spike of
381 $115 \mu\text{g/L}$. Upon cell lysis, the initially internalized Cr^{VI} would be released back to the test
382 medium resulting in an apparent stable total (dissolved) Cr concentration over the duration of
383 the experiment. Note that Cr^{VI} can undergo intracellular reduction to Cr^{III} (Cheung and Gu
384 2007; Volland et al. 2012; Kováčik et al. 2015) which could also be released back to the test
385 medium upon cell lysis; possibly in association with intracellular constituents preventing its
386 precipitation in the test medium. While no experiments were performed to determine if cell
387 lysis had occurred, we verified possible changes in the redox state of Cr in the test medium
388 over the exposure duration.

389 *Chromium redox speciation*

391 Aliquots of test medium spiked with Cr^{VI} exhibited a single peak, corresponding to the one
392 observed in a standard solution of Cr^{VI} , with a retention time of about 50 s regardless of the
393 presence of algae and of the incubation time (Figures 2A and S6). The total Cr^{VI}
394 concentration, determined from total peak area, was $118 \mu\text{g/L}$ at $t=0$ and $120 \mu\text{g/L}$ after 72h
395 of incubation in the abiotic test medium and $137 \mu\text{g/L}$ at $t=0$ and $120 \mu\text{g/L}$ after 72h in the
396 biotic medium. No peaks corresponding to Cr^{III} were observed in either abiotic or biotic test
397 medium (Figures 2A and S6). While this result does not provide information on possible Cr^{VI}
398 to Cr^{III} interconversion in the intracellular environment (Shanker et al. 2005; Viti et al. 2014;
399 Kováčik et al. 2015), it shows that algal cells are exposed to a practically constant
400 concentration of Cr^{VI} throughout the test duration. The corresponding ECs50 values for Cr^{VI}

401 can therefore be confidently ascribed to this specific redox form and calculated from the
402 concentrations initially added to the test medium.

403 On the other hand, marked and rapid changes in Cr speciation occurred in medium aliquots
404 amended with Cr^{III}. At t=0 and in the absence of algae, a single peak at a retention time of
405 about 100 s, corresponding to the hydrated Cr^{III} ion, was observed (Figure 2B). The
406 corresponding dissolved Cr^{III} concentration determined by IC-ICP-MS was 57 µg/L, in
407 agreement with the expected value of 60 µg/L. However, after 24 h of incubation, the peak
408 area at 100 s had dropped by 99% and the corresponding dissolved Cr^{III} concentration at 72 h
409 was only 0.39 µg/L (Figure 2B). Starting from 24 h after spiking, two additional peaks were
410 observed at retention times around 45 s and 75 s (Figure 2B). Considering the measured pH
411 range of the test medium (7.5–7.9 for medium aliquots amended with Cr^{III} concentrations
412 between 20 and 1250 µg Cr/L), Cr^{III} is expected to rapidly undergo hydrolysis (Rai et al.
413 1989; Richard and Bourg 1991; Kotaš and Stasicka 2000) and the peaks at 45 and 75 s likely
414 correspond to the hydrolytic Cr^{III} complexes Cr(OH)²⁺ and Cr(OH)₃⁰ (Séby et al.
415 2003). Addition of 5 µg/L of Cr^{VI} to an aliquot of the solution initially spiked with 60 µg/L of
416 Cr^{III} and aged for 4 h resulted in the expected Cr^{VI} peak at 50 s, thus confirming that the peak
417 at 45 s was not the results of an oxidation of Cr^{III} to Cr^{VI} during the experiment (Figures 2C
418 and S6).

419 As already seen in the previous section, for an initial concentration of 60 µg/L of Cr^{III},
420 speciation calculations using Visual Minteq suggest that, at equilibrium, the positively
421 charged species Cr(OH)₂⁺ and CrOH²⁺ should represent about 3.5% of the total in the
422 observed pH range of 7.8–7.9. Assuming a dissolved Cr concentration of 11 µg Cr/L after 72h
423 of incubation (see previous section and figure 1), the theoretical concentration of positively
424 charged Cr species at the end of the exposure period would be 0.2–0.4 µg/L; in agreement
425 with the IC-ICP-MS speciation results (Figure 2B).

426 Samples spiked with Cr^{III} in the presence of algae showed the three distinct peaks at retention
427 times of about 100 s, 75 s, and 45 s already at t = 0 (Figure S6). The area of all peaks rapidly
428 decreased and became practically negligible after 24 hours of incubation (Figure S6). In the
429 presence of algae, the concentration of hydrated Cr^{III} (peak at 100 s) decreased from 30 µg/L
430 at t = 0 to 0.14 µg/L at t = 72 h (Figure S6). The discrepancy between the measured (30 µg/L)
431 and expected concentration (60 µg/L) at t = 0 can be explained by a more rapid formation of
432 hydrolysis products. Indeed, the presence of particular microenvironments with increased pH
433 around algal cells and colonies was reported to enhance Fe hydrolysis (Sunda and Huntsman
434 2003) and an analogous phenomenon may occur in the case of Cr^{III}. Again, no peak indicative
435 of the formation of Cr^{VI} was identified throughout the experiment duration so that the
436 ecotoxicological effects discussed previously (section Chromium ecotoxicity in Results and
437 Discussion) can be ascribed to Cr^{III}.

438 The disappearance of the chromatographic peak of hydrated Cr^{III} (t = 100 s) between 0 and 24
439 h of incubation prompted us to examine the changes in Cr^{III} speciation at shorter time
440 intervals. Note that, given the absence of calibration standards for the peaks at 45 and 75 s,
441 the changes in the relative importance of the chromatographic peaks can be discussed solely
442 on the basis of their signal intensities. Immediately after spiking, 84% of dissolved Cr was
443 present as hydrated Cr^{III} (retention time 100 s) with the peaks at 75 s and 45 s representing
444 about 8% of the total signal each (Figures 2C and 3). The peak of hydrated ionic Cr^{III} at 100 s
445 decreased very rapidly and was only 2% of the initial dissolved Cr concentration after 6 hours
446 of incubation (Figure 3). At the same time, the peak at 75s increased up to 56% of the total
447 signal 1 hour after spiking and then slowly decreased to 40% after 6 h. The peak at 45 s
448 accounted for 7 and 10% of the total signal regardless of the incubation time (Figure 3). Both
449 the sum of the signals of the three peaks and the corresponding dissolved Cr signal (assayed

450 by ICP-MS) decreased by 50% and 40% compared with their respective initial values (Figure
451 3).

452 Samples collected after 24, 48, and 72 h of incubation confirmed the initial decreasing trend
453 and, in the case of dissolved Cr, were comparable with the results obtained by FAAS (Figure
454 1). The difference between dissolved Cr (ICP-MS) and the sum of various Cr peaks (IC-ICP-
455 MS) may be due to nanoparticle formation depositing in the column and going undetected. On
456 the other hand, the signal of total Cr (in terms of relative intensity measured by ICP-MS)
457 remained within 20% of the initial value (Figure 3). Overall, the rapid changes in Cr^{III}
458 speciation added to the test medium (particularly the disappearance of ionic Cr^{III} in less than 2
459 h) arise the question of which Cr^{III} species are actually responsible for the observed decrease
460 in algal biomass during ecotoxicity testing. These considerations will be developed later in the
461 text (section Implications for Cr hazard and risk assessment) after the presentation of the
462 results confirming the formation of Cr-bearing particles in the test medium.

463

464 *Formation of chromium (nano)particles*

465 NTA analysis showed that colloidal particles formed within minutes after adding soluble Cr^{III}
466 into the test medium. Particle concentration and size ranged between 9.64×10^8 and $29.7 \times$
467 10^8 particles/mL and 80 and 140 nm, respectively (Figure 4). The particle concentration was
468 $0.17 \pm 0.10 \times 10^8$ particles/mL in test medium without added Cr^{III} (Figure 4). Filtration (0.22
469 μm) of Cr^{III}-amended aliquots of test medium lowered particle concentration to around $0.6 \times$
470 10^8 particles/mL, but did not decrease their size by more than 25% (Figure 4). Total Cr
471 concentration remained within $\pm 20\%$ of initial value over the entire experiment duration.
472 Dissolved Cr concentrations also did not change during the first 2 h of incubation, but then
473 progressively decreased to 26% of the initial value after 72h (Figure 4). The concomitant
474 removal of particles and decrease in dissolved Cr concentration (Figure 4) confirms the
475 formation of Cr containing (nano)particles starting from initially soluble Cr^{III} salts for
476 incubation times > 24 h (Figure 4). The experimental decrease of dissolved Cr concentrations
477 is in agreement with the theoretical calculation performed with Visual Minteq (see Chromium
478 ecotoxicity in Results and discussion).

479 Analysis by spICP-MS confirmed that the nanoparticles formed immediately after spiking
480 actually contained Cr (Figure S11). The orders of magnitude of size is similar to those
481 measured using NTA (Figure S11 and Figure 4), at least when using the assumed composition
482 and shape (Table S3). On the other hand, spICP-MS detected an increase in particle number
483 from 5×10^6 ($t \leq 24$ h) to 2×10^8 ($t \geq 72$ h), suggesting that the mass percentage of Cr^{III}
484 occurring as particles increased from 4% at 0 h to 20% at 72 h to 76% at 96 h. Differences in
485 particle numbers estimated by spICP-MS and NTA likely arise from the specific technical
486 features of the two methods. Large particles do not manage to pass a spray chamber and are
487 therefore not measured during spICP-MS (Tuoriniemi et al. 2017), which therefore tends to
488 favor small particles as long as they are larger than the detection limit of approx. 90 nm.

489 NTA, in contrast, preferentially detects relatively large particles that scatter more light and is
490 less accurate in detecting relatively small particles. Note also that the particle size
491 distributions detected with spICP-MS abruptly stop at the size detection limit. Thus, despite
492 the two techniques yielding similar average particle sizes, NTA likely observes a fairly
493 constant number concentration of relatively large particles that are mostly removed by
494 filtration, while spICPMS observes an increase in the number of (relatively small) particles
495 with time (Figure 4 and S11). At short incubation times, a very large mass of Cr may reside in
496 the particle fraction that can pass a 0.22 μm filter without being detected by neither NTA nor
497 spICP-MS. Hence, a decrease Cr mass concentration is not observed when filtering samples at
498 0.22 μm at short incubation times (Figure 4). Measurement of total and dissolved Fe (data not
499 shown) allowed to exclude the formation of Fe-bearing particles (including mixed Cr-

500 Fe(oxy)hydroxides) (Sass and Rai 1987) and thus the possibility of indirect ecotoxic effect of
501 Cr^{III} via sequestration of the essential nutrient Fe. Interestingly, model calculations with
502 Visual Minteq predicted that the test medium should be oversaturated with respect to different
503 mineral phases including several Fe-containing minerals and hydroxyapatite. The exact
504 chemical nature of particles formed in Cr-spiked test medium clearly deserves further
505 experimental investigation, especially at short incubation times for which the assumption of
506 equilibrium is unlikely to be valid. Finally, removal of particles with sizes between 80 and
507 140 nm by filters with a 0.22 µm nominal cut-off can be explained by an actual smaller cut-
508 off of the filters' pores (She et al. 2008) or by the formation of larger particles undetectable
509 via NTA and spICP-MS.

510 Measurements by SPC confirmed the presence of particles in the same range identified by
511 NTA and spICP-MS, but also of particles larger than 300 nm in unfiltered test medium spiked
512 with Cr^{III} and incubated for 24, 48, and 72 hours (Figure 5 and S7). At t=0, only particles
513 between 50 and 150 nm were observed at a concentration of 3.2×10^5 particles/mL. After 24
514 hours, the concentration of particles between 50 and 200 nm increased to 6.1×10^6
515 particles/mL and particles larger than 300 nm (8.5×10^3 particles/mL) had also appeared.
516 Particles in the range 50–200 nm were still present after 48 (6.5×10^6 particles/mL) and 72 h
517 (9.8×10^6 particles/mL) of incubation, while particles larger than 300 nm eventually
518 disappeared after 72 h (Figure 5). The latter observation suggests the formation of particles
519 too large to be measured by the instruments or, more likely, settling too quickly to be
520 effectively sampled by the instrument.

521 Based on the analysis of total and dissolved Cr in the samples subject to SPC measurements
522 (figure S7), 45 µg of Cr (75% of the Cr^{III} initially added to the test medium) had been
523 incorporated in the observed particles after 72 hours. This result agrees well with the
524 corresponding Visual Minteq calculations (see section Cr ecotoxicity in Results and
525 discussion for details). Assuming a density of 3.11 g/cm³ for the amorphous Cr
526 oxyhydroxides likely occurring in the medium, the total volume of the particles would be
527 approx. 1.45×10^{-14} m³/mL. Given an approximate volume of 5.24×10^{-22} m³ for an
528 individual (spherical) particle with a diameter of 100 nm, a mass of Cr of 45 µg would be
529 enough to form 2.76×10^7 particles/mL. The presence of larger particles, unaccounted for in
530 the previous calculation, can be invoked to explain the difference between calculations and
531 SPC measurements.

532

533 *Implications for Cr hazard and risk assessment*

534 Our results show that Cr^{III} speciation into a standardized ecotoxicological test medium for
535 algae changes within a few hours after spiking; even when the total Cr^{III} concentration
536 remains comparatively stable. Similar, although less detailed, investigations on daphnids
537 (Ponti et al. 2014) and bacteria (Bencheikh-Latmani et al. 2007) suggest that such behavior
538 may be common in ecotoxicological media whose composition favors the formation of Cr^{III}
539 hydroxides. Thus, new ecotoxicological data for the hazard assessment of Cr^{III} must be
540 obtained by considering the recommendations originally developed for sparingly soluble
541 substances (ISO 14442 2006) [46]. In particular, in the case of marked differences (> 20%)
542 between nominal and actual concentration, the corresponding EC50 for Cr^{III} must be
543 calculated as the TWM of the dissolved concentration (OECD 2012). The excellent agreement
544 between experimental results and thermodynamic modeling of speciation equally suggests
545 that our observations could have a broader validity, although the kinetics of temporal
546 speciation changes may vary across media and as a function of initial Cr^{III} concentration.
547 Furthermore, following our IC-ICPMS results, the question of the actual Cr^{III} species
548 responsible for the observed ecotoxicological effects in living organisms deserves additional
549 study. An application of the biotic ligand model to the study of root elongation in barley

550 (Song et al. 2014) suggested Cr^{3+} and $\text{Cr}(\text{OH})^{2+}$ as the two biologically active chemical
551 species in controlling the effects of Cr^{III} . However, the rapid disappearance (< 2 h) of ionic Cr
552 from the test medium questions the role of such species in determining the observed algal
553 response. One possibility is that a pulse exposure to $60 \mu\text{g/L}$ of truly dissolved Cr^{III} at the
554 beginning of the test can cause a 50% reduction in algal biomass after incubation over 72 h.
555 Alternatively, the residual concentration of ionic Cr^{III} after 2 h (less than $1 \mu\text{g/L}$) determines
556 the effect observed at the end of the test or the other Cr^{III} species also contribute to the
557 observed toxicity. The formation of some Cr-bearing (nano)particles over the course of the
558 test also points to a possible nano-ecotoxicological dimension in the toxicity of Cr^{III} to algae.
559 In particular, freshly formed $\text{Cr}(\text{OH})_3$ particles can lead to the formation of “transiently
560 available Cr^{III} species” which may be highly toxic (Bencheikh-Latmani et al. 2007). The
561 existence of monomeric and polymeric Cr^{III} being documented in environmental samples (Hu
562 et al. 2016), both Cr hydroxides and Cr-bearing (nano)particles may have an ecotoxicological
563 role outside laboratory settings and deserve consideration in risk assessment for Cr^{III} .
564 The present study does not question the high ecotoxicity of Cr^{VI} , but it adds to the growing
565 evidence that the biological effects of Cr^{III} strongly depend on the composition of the medium
566 used for testing and are likely underestimated (Lira-Silva et al. 2011; Ponti et al. 2014). In this
567 context, the paradigm ‘ Cr^{VI} is more toxic than Cr^{III} ’ increasingly appears as an oversimplified
568 representation of environmental reality. In this context, more detailed studies on the
569 speciation Cr^{III} in standardized ecotoxicological laboratory settings are highly desirable for at
570 least three reasons. First, reduction of Cr^{VI} to Cr^{III} is a typical strategy for remediation of Cr-
571 contaminated matrices and environments; second Cr contamination remains a serious
572 environmental problem in several low to middle income countries whose economic activity is
573 linked with the material demands of the current lifestyle in developed countries (Pure Earth
574 and Green Cross 2016); third the safe perspective use of Cr_2O_3 nanoparticles is linked to their
575 intrinsic properties, but also to the possible release of soluble Cr in either redox forms (Horie
576 et al. 2013; da Costa et al. 2016; Puerari et al. 2016). In all cases, the appropriate knowledge
577 of the actual ecotoxicity of Cr^{VI} and Cr^{III} necessary to assess the environmental risks of Cr
578 appears incomplete. Identifying the exact chemical species responsible for ecotoxicological
579 effects, especially in the case of Cr^{III} , will facilitate extrapolation of laboratory findings to
580 complex environmental realities and the associated remediation/management decision.

581
582 *Supplemental data*— The Supplemental Data are available on the Wiley Online Library at
583 DOI: 10.1002/etc.xxx. Details for IC-ICP-MS experiments and analytical procedures,
584 temporal evolution of dissolved Cr^{III} and Cr^{VI} concentrations, complementary IC-ICP-MS
585 results, optimization and details of NTA and spICP-MS procedures and additional
586 measurements of particle size distribution and number by SPC, NTA and spICP-MS.

587 588 *Acknowledgment*

589 This work is part of the PhD thesis of I. Aharchaou who is supported by the French Ministry
590 of Education. The financial support of the CNRS (project EC2CO Insokintox) is greatly
591 acknowledged. We thank A. Garnier (LHN, ANSES, Nancy) for help with IC-ICP-MS
592 analysis. The contributions of S. Cambier were in part made possible within NANION
593 (FNR/12/SR/4009651-Fonds National de la Recherche Luxembourg). We are grateful to E.
594 Szalinska (AGH University of Science and Technology, Krakow, Poland) for her help in
595 some experiments. D. Vignati and G. Cornelis acknowledge the support of COST action
596 ES1205 (STSM 35421).

597

598 **REFERENCES**

- 599 Anses. Méthode d'analyse du chrome hexavalent dans les eaux. [accessed 2016 Apr 11].
600 <https://www.anses.fr/fr/system/files/MethodeChromeHexavalentEaux-Consultation.pdf>.
601
- 602 Bencheikh-Latmani R, Obraztsova A, Mackey MR, Ellisman MH, Tebo BM. 2007. Toxicity
603 of Cr(III) to *Shewanella sp.* Strain MR-4 during Cr(VI) Reduction. Environ. Sci. Technol.
604 41:214–220. doi:10.1021/es0622655.
605
- 606 Bobrowski A, Baś B, Dominik J, Niewiara E, Szalińska E, Vignati D, Zarbski J. 2004.
607 Chromium speciation study in polluted waters using catalytic adsorptive stripping
608 voltammetry and tangential flow filtration. Talanta 63:1003–1012.
609 doi:10.1016/j.talanta.2004.01.004.
610
- 611 Carr , B, Wright, M. 2013. Nanoparticle Tracking Analysis. [accessed 2016 Mar 21].
612 http://particularsciences.ie/psl/brochures/supplier_brochures_pdf/nta_brochure.pdf.
613
- 614 Chapman GA, Ota S, Recht F, Corvallis Environmental Research Laboratory. 1980. Effects of
615 water hardness on the toxicity of metals to *Daphnia magna*: status report - January 1980.
616 Corvallis, Ore.: U.S. Environmental Protection Agency, Corvallis Environmental Research
617 Laboratory.
618
- 619 Cheung KH, Gu J-D. 2007. Mechanism of hexavalent chromium detoxification by
620 microorganisms and bioremediation application potential: A review. Int. Biodeterior.
621 Biodegrad. 59:8–15. doi:10.1016/j.ibiod.2006.05.002.
622
- 623 da Costa CH da, Perreault F, Oukarroum A, Melegari SP, Popovic R, Matias WG. 2016.
624 Effect of chromium oxide (III) nanoparticles on the production of reactive oxygen species and
625 photosystem II activity in the green alga *Chlamydomonas reinhardtii*. Sci. Total Environ.
626 565:951–960. doi:10.1016/j.scitotenv.2016.01.028.
627
- 628 Dazy M, Béraud E, Cotelle S, Meux E, Masfaraud J-F, Férard J-F. 2008. Antioxidant enzyme
629 activities as affected by trivalent and hexavalent chromium species in *Fontinalis antipyretica*
630 Hedw. Chemosphere 73:281–290. doi:10.1016/j.chemosphere.2008.06.044.
631
- 632 de Paiva Magalhães D, da Costa Marques MR, Baptista DF, Buss DF. 2015. Metal
633 bioavailability and toxicity in freshwaters. Environmental Chemistry Letters 13:69–87.
634
- 635 Didur O, Dewez D, Popovic R. 2013. Alteration of chromium effect on photosystem II
636 activity in *Chlamydomonas reinhardtii* cultures under different synchronized state of the cell
637 cycle. Environ. Sci. Pollut. Res. 20:1870–1875. doi:10.1007/s11356-012-1389-8.
638
- 639 Dominik J, Vignati D a. L, Koukal B, Pereira de Abreu M-H, Kottelat R, Szalinska E, Baś B,
640 Bobrowski A. 2007. Speciation and Environmental Fate of Chromium in Rivers
641 Contaminated with Tannery Effluents. Eng. Life Sci. 7:155–169.
642 doi:10.1002/elsc.200620182.
643
- 644 Vindimian.E. 2010. REGTOX: macro Excel™ for dose-response modelling.
645
- 646 Fairbrother A, Wenstel R, Sappington K, Wood W. 2007. Framework for Metals Risk
647 Assessment. Ecotoxicol. Environ. Saf. 68:145–227. doi:10.1016/j.ecoenv.2007.03.015.

648
649 Harris CA, Scott AP, Johnson AC, Panter GH, Sheahan D, Roberts M, Sumpter JP. 2014.
650 Principles of Sound Ecotoxicology. *Environ. Sci. Technol.* 48:3100–3111.
651 doi:10.1021/es4047507.
652
653 Holdway D. 1988. The toxicity of chromium to fish. In Nriagu JO, Nieboer E, eds, *Chromium*
654 *in the natural and human environments.* John Wiley & Sons, pp. 369–397.
655
656 Horie M, Nishio K, Endoh S, Kato H, Fujita K, Miyauchi A, Nakamura A, Kinugasa S,
657 Yamamoto K, Niki E, et al. 2013. Chromium(III) oxide nanoparticles induced remarkable
658 oxidative stress and apoptosis on culture cells. *Environ. Toxicol.* 28:61–75.
659 doi:10.1002/tox.20695.
660
661 Hu L, Cai Y, Jiang G. 2016. Occurrence and speciation of polymeric chromium(III),
662 monomeric chromium(III) and chromium(VI) in environmental samples. *Chemosphere*
663 156:14–20. doi:10.1016/j.chemosphere.2016.04.100.
664
665 Munn S. J Allanou, R Aschberger, K Berthault, F Cosgrove, O Luotamo, M Vegro. 2005.
666 Chromium trioxide, sodium chromate, sodium dichromate, ammonium dichromate, potassium
667 dichromate, EUR 21508 EN. *European Union Risk Assessment Report*, 53..
668
669 ISO 14442. 2006. Water quality -- Guidelines for algal growth inhibition tests with poorly
670 soluble materials, volatile compounds, metals and waste water.
671 Kotaš J, Stasicka Z. 2000. Chromium occurrence in the environment and methods of its
672 speciation. *Environ. Pollut.* 107:263–283. doi:10.1016/S0269-7491(99)00168-2.
673
674 Kováčik J, Babula P, Hedbavny J, Kryštofová O, Provazník I. 2015. Physiology and
675 methodology of chromium toxicity using alga *Scenedesmus quadricauda* as model object.
676 *Chemosphere* 120:23–30. doi:10.1016/j.chemosphere.2014.05.074.
677
678 Labra M, Bernasconi M, Grassi F, De Mattia F, Sgorbati S, Airoidi R, Citterio S. 2007. Toxic
679 and genotoxic effects of potassium dichromate in *Pseudokirchneriella subcapitata* detected
680 by microscopy and AFLP marker analysis. *Aquat. Bot.* 86:229–235.
681 doi:10.1016/j.aquabot.2006.10.006.
682
683 Lin C-J. 2002. The Chemical Transformations of Chromium in Natural Waters – A Model
684 Study. *Water. Air. Soil Pollut.* 139:137–158. doi:10.1023/A:1015870907389.
685
686 Lira-Silva E, Ramírez-Lima IS, Olín-Sandoval V, García-García JD, García-Contreras R,
687 Moreno-Sánchez R, Jasso-Chávez R. 2011. Removal, accumulation and resistance to
688 chromium in heterotrophic *Euglena gracilis*. *J. Hazard. Mater.* 193:216–224.
689 doi:10.1016/j.jhazmat.2011.07.056.
690
691 Liu J, Fu J, Ning X 'an, Sun S, Wang Y, Xie W, Huang S, Zhong S. 2015. An experimental
692 and thermodynamic equilibrium investigation of the Pb, Zn, Cr, Cu, Mn and Ni partitioning
693 during sewage sludge incineration. *J. Environ. Sci.* 35:43–54. doi:10.1016/j.jes.2015.01.027.
694
695 Mason RP. 2013. *Trace Metals in Aquatic Systems.* John Wiley & Sons.
696

697 Masscheleyn PH, Pardue JH, DeLaune RD, Patrick J WH. 1992. Chromium Redox Chemistry
698 in a Lower Mississippi Valley Bottomland Hardwood Wetland. *Environ. Sci. Technol.*
699 26:1217–1226. doi:10.1021/es50002a611.
700

701 Morel, F.M.M. 1983. *Principles of Aquatic Chemistry*. Wiley, New York.
702

703 OECD. 2011. Test No. 201: Freshwater Alga and Cyanobacteria, Growth Inhibition Test.
704 Paris: Organisation for Economic Co-operation and Development. [accessed 2015 Sep 18].
705 <http://www.oecd-ilibrary.org/content/book/9789264069923-en>.
706

707 OECD. 2012. Test No. 211: *Daphnia magna* Reproduction Test. Paris: Organisation for
708 Economic Co-operation and Development. [accessed 2015 Sep 18]. [http://www.oecd-](http://www.oecd-ilibrary.org/content/book/9789264185203-en)
709 [ilibrary.org/content/book/9789264185203-en](http://www.oecd-ilibrary.org/content/book/9789264185203-en).
710

711 World Health Organization. 2009. Inorganic Chromium(III) Compounds.
712

713 World Health Organization. 2013. Inorganic Chromium(VI) Compounds.
714

715 Pace HE, Rogers NJ, Jarolimek C, Coleman VA, Higgins CP, Ranville JF. 2011. Determining
716 Transport Efficiency for the Purpose of Counting and Sizing Nanoparticles via Single Particle
717 Inductively Coupled Plasma Mass Spectrometry. *Anal. Chem.* 83:9361–9369.
718 doi:10.1021/ac201952t.
719

720 Ponti B, Bettinetti R, Dossi C, Vignati DAL. 2014. How reliable are data for the ecotoxicity
721 of trivalent chromium to *Daphnia magna*? *Environ. Toxicol. Chem.* 33:2280–2287.
722 doi:10.1002/etc.2672.
723

724 Puerari RC, da Costa CH, Vicentini DS, Fuzinato CF, Melegari SP, Schmidt ÉC, Bouzon ZL,
725 Matias WG. 2016. Synthesis, characterization and toxicological evaluation of Cr₂O₃
726 nanoparticles using *Daphnia magna* and *Aliivibrio fischeri*. *Ecotoxicol. Environ. Saf.* 128:36–
727 43. doi:10.1016/j.ecoenv.2016.02.011.
728

729 Pure Earth, Green Cross. 2016. *The World’s Worst Pollution Problems 2016: The Toxics*
730 *Beneath Our Feet*. [accessed 2016 Nov 19].
731

732 Rai D, Eary LE, Zachara JM. 1989. Environmental chemistry of chromium. *Sci. Total*
733 *Environ.* 86:15–23. doi:10.1016/0048-9697(89)90189-7.
734

735 Richard FC, Bourg ACM. 1991. Aqueous geochemistry of chromium: A review. *Water Res.*
736 25:807–816. doi:10.1016/0043-1354(91)90160-R.
737

738 Rossé P, Loizeau J-L. 2003. Use of single particle counters for the determination of the
739 number and size distribution of colloids in natural surface waters. *Colloids Surf.*
740 *Physicochem. Eng. Asp.* 217:109–120. doi:10.1016/S0927-7757(02)00565-4.
741

742 Sacher F, Raue B, Klinger J, Brauch H-J. 1999. Simultaneous Determination of Cr(III) and
743 Cr(VI) in Ground and Drinking Waters by IC-ICP-MS. *Int. J. Environ. Anal. Chem.* 74:191–
744 201. doi:10.1080/03067319908031425.
745

746 Saputro S, Yoshimura K, Matsuoka S, Takehara K, Narsito, Aizawa J, Tennichi Y. 2014.
747 Speciation of dissolved chromium and the mechanisms controlling its concentration in natural
748 water. *Chem. Geol.* 364:33–41. doi:10.1016/j.chemgeo.2013.11.024.
749

750 Sass BM, Rai D. 1987. Solubility of amorphous chromium(III)-iron(III) hydroxide solid
751 solutions. *Inorg. Chem.* 26:2228–2232. doi:10.1021/ic00261a013.
752

753 Séby F, Charles S, Gagean M, Garraud H, Donard OFX. 2003. Chromium speciation by
754 hyphenation of high-performance liquid chromatography to inductively coupled plasma-mass
755 spectrometry—study of the influence of interfering ions. *J. Anal. At. Spectrom.* 18:1386–
756 1390. doi:10.1039/B306249J.
757

758 Shanker AK, Cervantes C, Loza-Tavera H, Avudainayagam S. 2005. Chromium toxicity in
759 plants. *Environ. Int.* 31:739–753. doi:10.1016/j.envint.2005.02.003.
760

761 She FH, Tung KL, Kong LX. 2008. Calculation of effective pore diameters in porous
762 filtration membranes with image analysis. *Robot. Comput.-Integr. Manuf.* 24:427–434.
763 doi:10.1016/j.rcim.2007.02.023.
764

765 Song N, Zhong X, Li B, Li J, Wei D, Ma Y. 2014. Development of a Multi-Species Biotic
766 Ligand Model Predicting the Toxicity of Trivalent Chromium to Barley Root Elongation in
767 Solution Culture. *PLoS ONE* 9:e105174. doi:10.1371/journal.pone.0105174.
768

769 Sunda W, Huntsman S. 2003. Effect of pH, light, and temperature on Fe–EDTA chelation and
770 Fe hydrolysis in seawater. *Mar. Chem.* 84:35–47. doi:10.1016/S0304-4203(03)00101-4.
771

772 Thompson SL, Manning FCR, McColl SM. 2002. Comparison of the Toxicity of Chromium
773 III and Chromium VI to Cyanobacteria. *Bull. Environ. Contam. Toxicol.* 69:286–293.
774 doi:10.1007/s00128-002-0059-9.
775

776 Tuoriniemi J, Cornelis G, Hassellöv M. 2015. A new peak recognition algorithm for detection
777 of ultra-small nano-particles by single particle ICP-MS using rapid time resolved data
778 acquisition on a sector-field mass spectrometer. *J. Anal. At. Spectrom.* 30:1723–1729.
779 doi:10.1039/C5JA00113G.
780

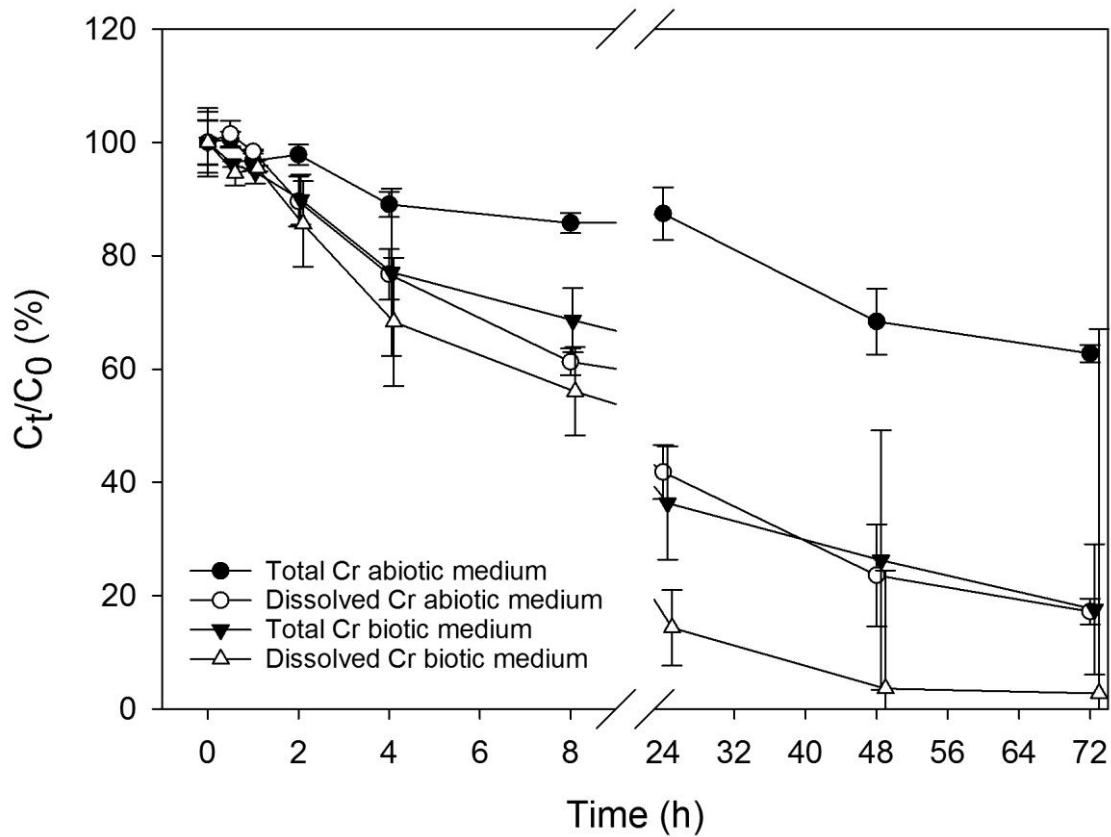
781 Tuoriniemi J, Jürgens MD, Hassellöv M, Cornelis G. 2017. Size dependence of silver
782 nanoparticle removal in a wastewater treatment plant mesocosm measured by FAST single
783 particle ICP-MS. *Environ. Sci. Nano* 4:1189–1197. doi:10.1039/C6EN00650G.
784

785 Vignati DAL, Beye ML, Dominik J, Klingemann AO, Filella M, Bobrowski A, Ferrari BJ.
786 2008. Temporal Decrease of Trivalent Chromium Concentration in a Standardized Algal
787 Culture Medium: Experimental Results and Implications for Toxicity Evaluation. *Bull.*
788 *Environ. Contam. Toxicol.* 80:305–310. doi:10.1007/s00128-008-9379-8.
789

790 Vignati DAL, Dominik J, Beye ML, Pettine M, Ferrari BJD. 2010. Chromium(VI) is more
791 toxic than chromium(III) to freshwater algae: A paradigm to revise? *Ecotoxicol. Environ. Saf.*
792 73:743–749. doi:10.1016/j.ecoenv.2010.01.011.
793

794 Viti C, Marchi E, Decorosi F, Giovannetti L. 2014. Molecular mechanisms of Cr(VI)
795 resistance in bacteria and fungi. *FEMS Microbiol. Rev.* 38:633–659. doi:10.1111/1574-
796 6976.12051.
797
798 Volland S, Lütz C, Michalke B, Lütz-Meindl U. 2012. Intracellular chromium localization
799 and cell physiological response in the unicellular alga *Micrasterias*. *Aquat. Toxicol.* 109:59–
800 69. doi:10.1016/j.aquatox.2011.11.013.
801
802
803
804
805
806
807
808
809

810 **Figure 1.**

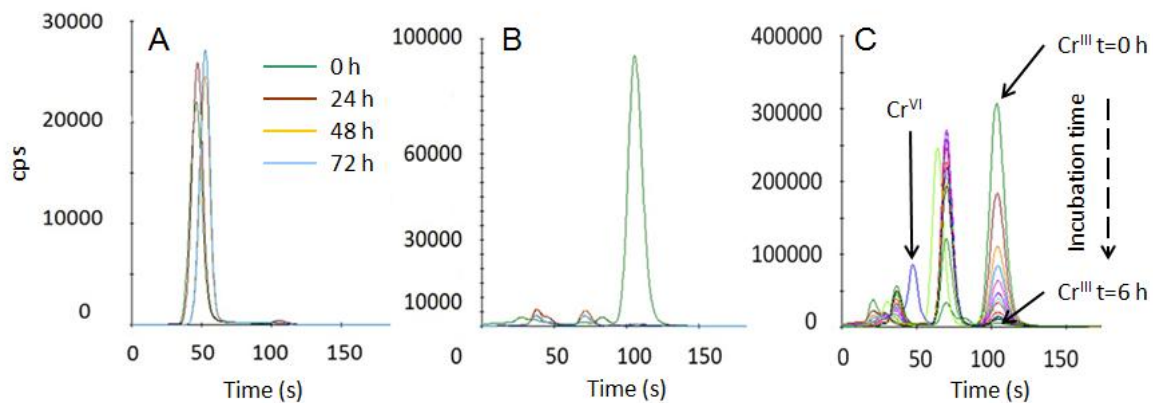


811
812
813 **Figure 1.** Temporal evolution (expressed as percentage of the value measured at $t = 0$) of total
814 and dissolved ($< 0.22 \mu\text{m}$) Cr concentrations in ISO medium amended with $\text{CrCl}_3 \cdot 6\text{H}_2\text{O}$ at an
815 initial concentration of $60 \mu\text{g Cr/L}$ (nominal value). Error bars indicate one standard deviation
816 (SD). Large SD after 72 h of incubation were caused by Cr concentration decreasing to values
817 close to the instrumental detection limit. C_0 and C_t refer to total or dissolved Cr concentration
818 measured at $t=0$ and at the various incubation times, respectively. All data points were
819 calculated on the basis of measured total and dissolved Cr values. The measured pH was 7.8–
820 7.9 over the entire duration of the experiment. Data points for different incubation times were
821 slightly nudged to visualize the corresponding error bars.

822
823
824
825
826
827
828
829
830
831
832
833

834 **Figure 2.**

835



836

837

838

839 **Figure 2.** Chromatograms of test medium (without added algae) at different incubation times.
840 Panels A and B: test medium amended with 115 $\mu\text{g/L}$ of Cr^{VI} ($\text{K}_2\text{Cr}_2\text{O}_7$) (A) or 60 $\mu\text{g/L}$ of
841 Cr^{III} ($\text{CrCl}_3 \cdot 6\text{H}_2\text{O}$) (B) at 0 h, 24 h, 48 h or 72 h after spiking. Panel C: temporal evolution of
842 chromatograms of test medium containing 60 $\mu\text{g/L}$ of Cr^{III} with measurements performed
843 every 20 min during 6 h. Note the peak of added Cr^{VI} (5 $\mu\text{g/L}$) at 50 s. All solutions were
844 filtered (0.22 μm) immediately before analysis; cps (counts per second). Note the different
845 scales on the y axes.

846

847

848

849

850

851

852

853

854

855

856

857

858

859

860

861

862

863

864

865

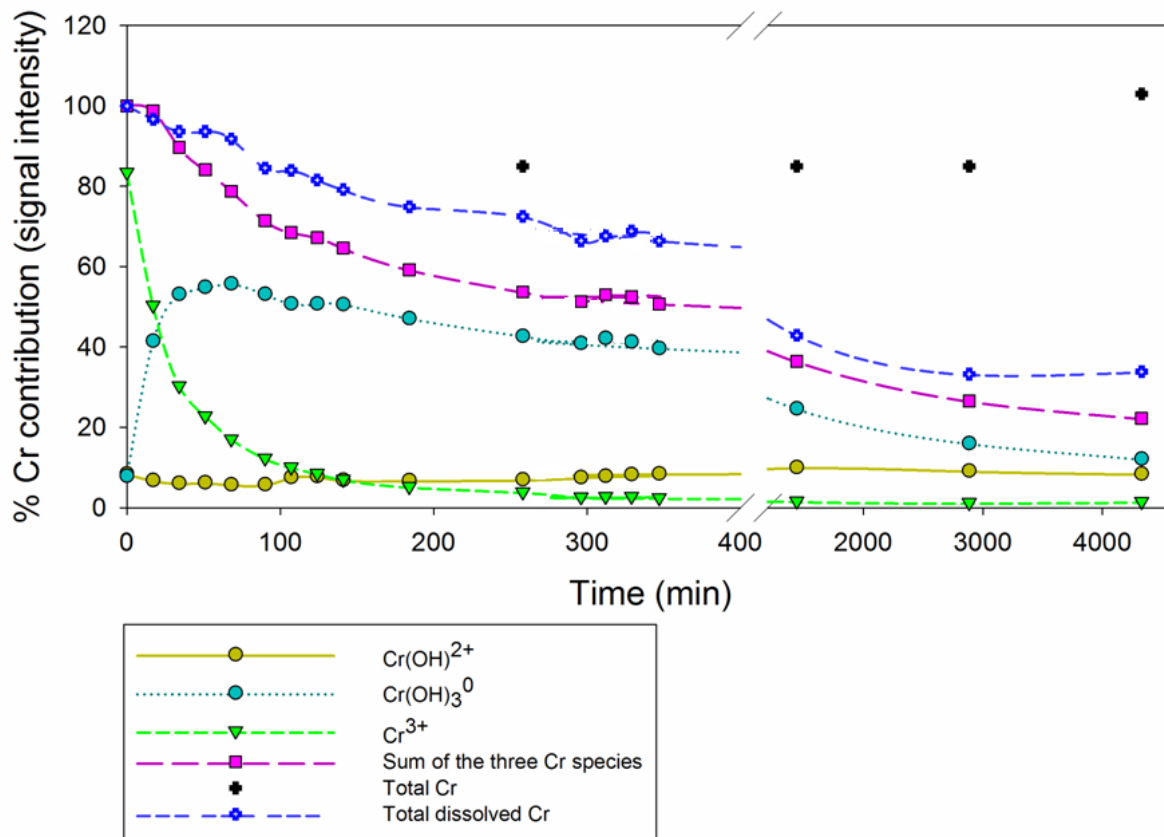
866

867

868

869 **Figure 3.**

870



871

872

873 **Figure 3.** Temporal evolution of the relative abundances of three Cr^{III} species (Cr(OH)²⁺,
874 yellow circles; Cr(OH)₃⁰, turquoise circles; Cr³⁺, green triangles) in ISO medium spiked with
875 60 µg Cr/L of Cr^{III} (CrCl₃·6H₂O) determined by IC-ICP-MS. The sum of the three Cr species
876 (pink squares) and the signals of total chromium (black crosses) and total dissolved chromium
877 (filtered at 0.22 µm; blue crosses) are also indicated.

878

879

880

881

882

883

884

885

886

887

888

889

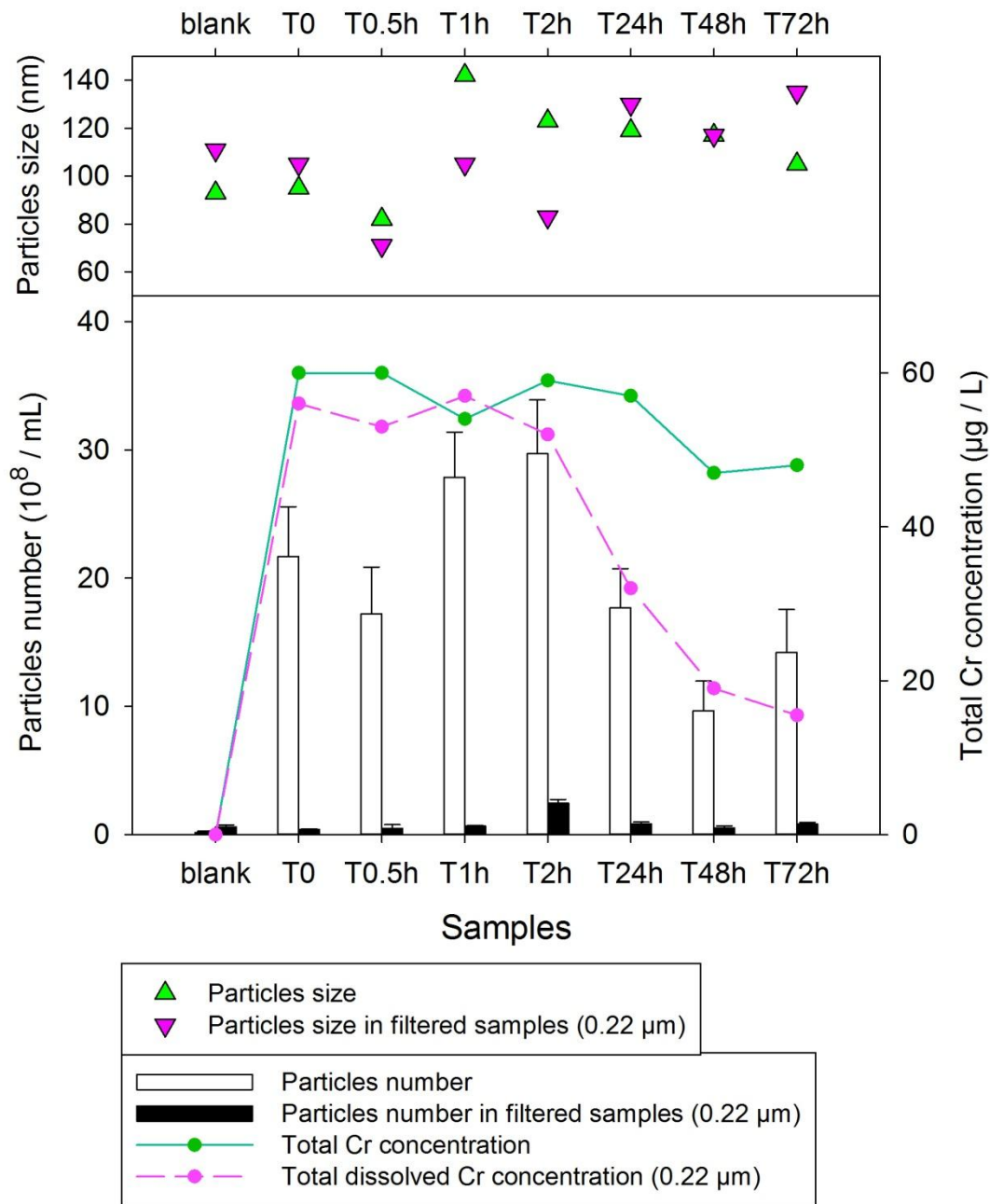
890

891

892

893 **Figure 4.**

894



895

896

897 **Figure 4.** Particle concentrations (bars), particle size (triangles) and Cr concentration (lines)

898 in unfiltered and filtered (0.22 µm) aliquots of ISO medium spiked (except for the sample

899 'Blank') with 60 µg/L of Cr^{III} (CrCl₃ · 6H₂O) at different incubation times. Particle

900 concentration and size measured by nanoparticle tracking analysis, Cr concentration measured

901 by atomic absorption spectrometry.

902

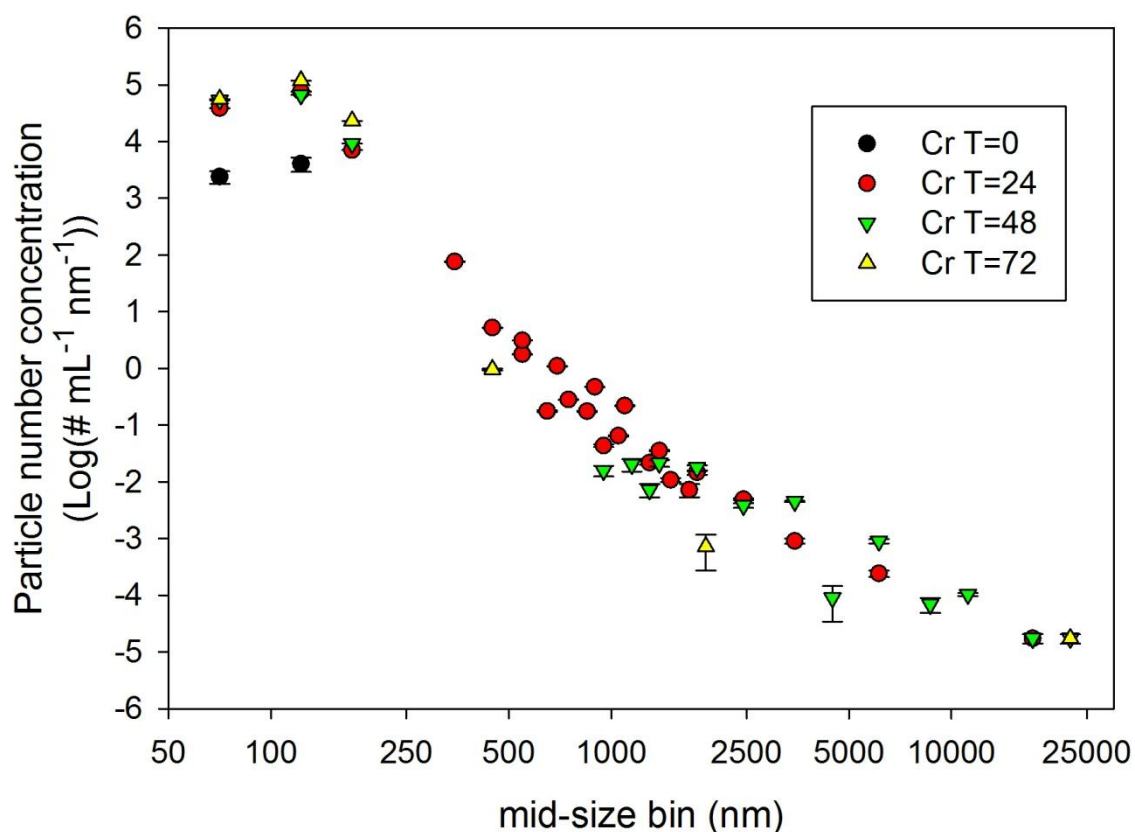
903

904

905

906

907 **Figure 5.**



908
909

910 **Figure 5.** Particle size distribution and number of particles (in mL⁻¹ nm⁻¹) in test medium
911 spiked with Cr^{III} (CrCl₃· 6H₂O) after 0 (black circles), 24 (red circles), 48 (green triangles)
912 and 72 h (yellow triangles) of incubation. All measurements were performed by Single
913 Particle Counter (SPC) at a sample flow rate of 64 mL/min. Results for each size class have
914 been corrected for particle concentration in ISO medium without added Cr^{III} (see figure S7 for
915 the corresponding comparisons). To obtain the number of particles per mL in a given size
916 range, the values on the y-axis must be multiplied for the corresponding size range (in nm) on
917 the x-axis.

918
919
920
921
922
923
924
925
926
927
928
929
930

Supporting information

931
932
933
934
935
936
937
938
939
940
941
942
943
944
945
946
947
948
949
950
951
952

953
954

955

956

957

958

959

960

961

962

963

964

965

966

Chromium speciation in a standardized ecotoxicological medium:
implications for hazard and risk assessment

Imad Aharchaou^{a*}, Jean-Sébastien Py^b, Sébastien Cambier^c, Jean-Luc Loizeau^d, Geert
Cornelis^e, Philippe Rousselle^a, Eric Battaglia^a, Davide A.L. Vignati^a

^a Laboratoire Interdisciplinaire des Environnements Continentaux LIEC-UMR 7360, Université de Lorraine and
CNRS, 8 rue du Général Delestraint, 57070 Metz, France

^b Agence nationale de sécurité sanitaire de l'alimentation, de l'environnement et du travail ANSES-Laboratoire
d'hydrologie de Nancy, 40 rue Lionnois, 54000 Nancy, France

^c Luxembourg Institute of Science and Technology LIST, 4 avenue des hauts fourneaux-L-4362 Esch
sur Alzette, Luxembourg

^d Institute François-Alphonse Forel and Institute for Environmental Sciences, University of Geneva, 66 Bd Carl-
Vogt, CH-1211 Genève, Switzerland

^e SLU Institutionen for vatten och miljo Lennart Hjelm's väg 9, Uppsala, SE 750 07, Sweden

Twelve supplementary figures and three supplementary tables

967 **Contents – Supporting information :**

968 Figure S1: Experimental plan for Cr speciation experiments with Ion Chromatography ICP-MS (IC-
969 ICP-MS)

970 Table S1: Summary of the IC-ICP-MS parameters and conditions used in Cr speciation experiments

971 Figure S2: Temporal evolution of two Cr^{III} initial concentrations (total dissolved) in ISO8692 medium
972 over 72 h

973 Figure S3: Temporal evolution of nine Cr^{III} initial concentrations (total dissolved) in ISO8692 medium
974 over 72 h

975 Figure S4: Temporal evolution of nine Cr^{III} initial concentrations (total) in ISO8692 medium over 72 h

976 Table S2: Measured Cr concentration at t = 0 in standard (ISO 8692) medium amended with different
977 initial concentrations with and without filtration

978 Figure S5: Temporal evolution of Cr^{VI} concentrations (CE₅₀ as added initial concentration) with and
979 without filtration in biotic (presence of algae) ISO medium.

980 Figure S6: Chromatograms of standard ISO 8692 biotic (presence of algae) medium amended with
981 Cr^{VI} or with Cr^{III} at different times between 0 and 72 h

982 Figure S7: Particle size distribution and number of particles determined with Single Particles Counter
983 in ISO algal test medium with and without addition of Cr^{III} at different incubation times

984 Figure S8: Particle size distribution and number of particles determined with Nanoparticle Tracking
985 Analysis in ISO algal test medium with and without addition of Cr^{III} at different incubation times

986 Figure S9: Nanoparticle Tracking Analysis results profiles before and after measurement parameters
987 modification.

988 Figure S10: Temporal evolution of chromium concentrations with and without filtration in ISO
989 medium amended with Cr^{III} during 72 hours.

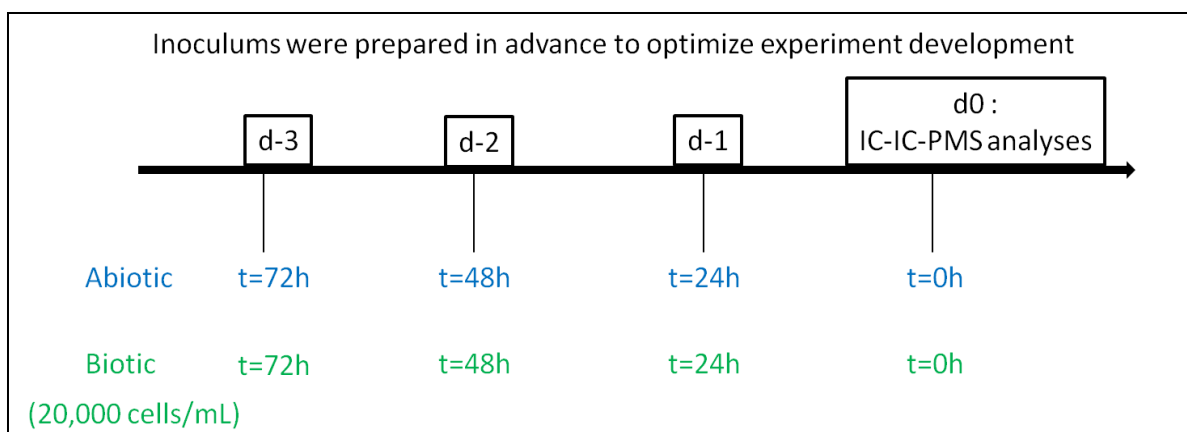
990 Table S3: Conditions and ICP-MS parameters for spICP-MS analysis.

991 Figure S11: Temporal evolution of particle number and % of total mass occurring as particle mass or
992 Number average and mass average particle diameter.

993 Figure S12: Time-dependent changes in the distribution of the corresponding spherical diameter.

994

995

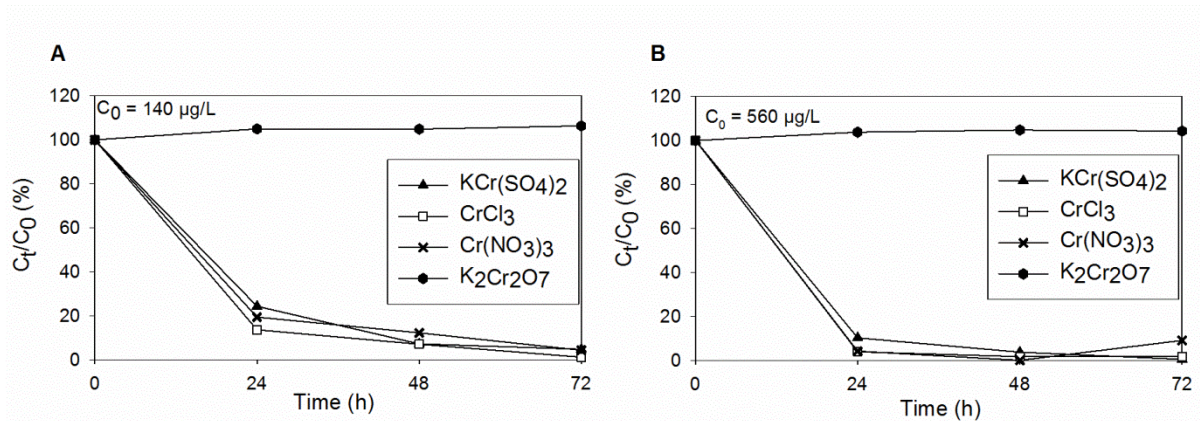


996

997 Figure S1. Experimental plan for speciation experiments with Ion Chromatography ICP-MS (IC-ICP-
 998 MS). Abiotic (absence of algae) and biotic (presence of algae) samples were prepared in advance or
 999 immediately prior to analysis (d0). All samples were analyzed on day 0 to optimize the analyses
 1000 course in day 0.

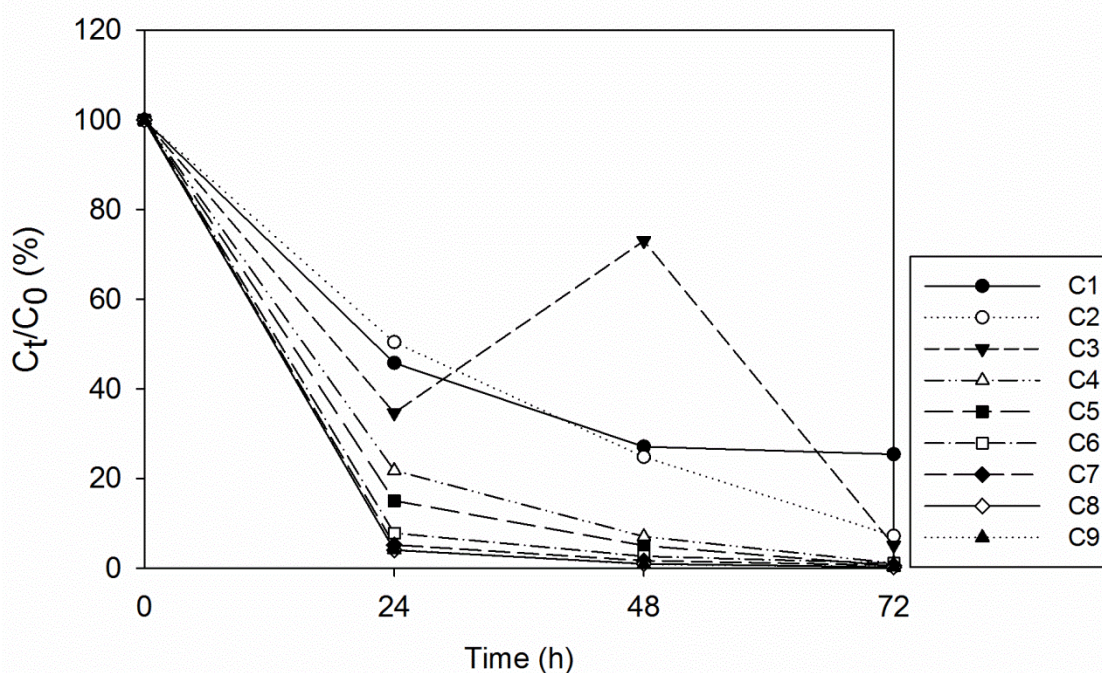
1001 Table S1: Summary of the IC-ICP-MS parameters and conditions used in Cr speciation experiments

IC conditions	
pump	Thermo ICS 5000+
separation column	Dionex Thermo AG7 2x50 mm
column temperature	20 °C
eluent	0.4 mol/L HNO ₃ spiked with 1µg/L of Rh, isocratic system
flow rate	500 µL/min
sample volume	200 µL
flushing volume	1,500 µL
duration	10 min
ICP-MS parameters	
ICP-MS	Thermo XII series
nebulizer	PFA-LC
gas flow	0.87 L/min
plasma power	1,500 W
plasma gas flow	13.5 L/min
auxiliary gas flow	0.77 L/min
detector mode	pulse counting
KED	He/H ₂
CCT – KED flow rate	3.5 mL/min – 3 V
Data acquisition	
ions (m/z)	⁵² Cr, ⁵³ Cr, ¹⁰³ Rh
measurement unit	counts
sweeps/reading	1
replicates	1
dwel time	100 ms
integration time	600,000 ms



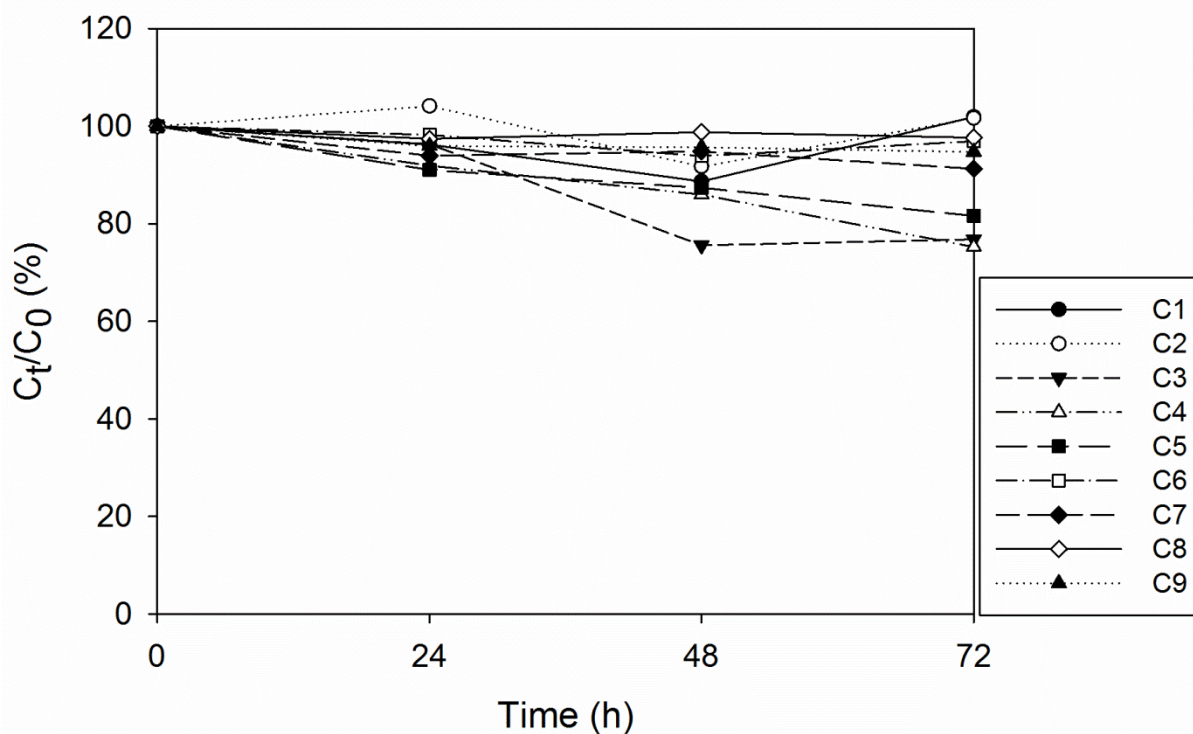
1002
 1003 Figure S2. Temporal evolution (expressed as a percentage of the value measured at t=0) of total
 1004 dissolved Cr concentrations (filtered at 0.22 µm) in standard (ISO8692) medium amended with Cr^{III}
 1005 (CrCl₃·6H₂O (square) or Cr(NO₃)₃·9H₂O (cross) or KCr(SO₄)₂·12H₂O (triangle)) or Cr^{VI} (K₂Cr₂O₇
 1006 (circle)) during 72 hours. Initial concentration of each salt was 140 µg/L (A) or 560 µg/L (B).

1007
 1008
 1009
 1010
 1011
 1012
 1013
 1014
 1015
 1016
 1017
 1018
 1019
 1020
 1021
 1022



1023
 1024 Figure S3. Temporal evolution (expressed as a percentage of the value measured at t=0) of total
 1025 dissolved Cr concentrations (filtered at 0.22 μm) in standard (ISO 8692) medium amended with initial
 1026 total concentrations of $\text{CrCl}_3 \cdot 6\text{H}_2\text{O}$ between 20 (C1) and 7000 (C9) $\mu\text{g/L}$ (see Table S2 for the full
 1027 compilation of the measured values at t = 0). Measurements were done in triplicate for C1, C2, C4 and
 1028 C9 after 0 and 48 h of incubation. The relative standard deviations (RSD) for these measurements
 1029 were usually below 10 % except for C1 at 48 h (RSD = 70%) and C2 at 48 h (RSD = 40%) and C3 at
 1030 48 h (RSD = 20%). The high RSD were obtained for analytical concentrations close to the
 1031 instrumental quantification limit for FAAS. Also note that, with increasing concentrations, total
 1032 dissolved Cr levels were lower than the corresponding total ones already at t = 0 (see Table S2).

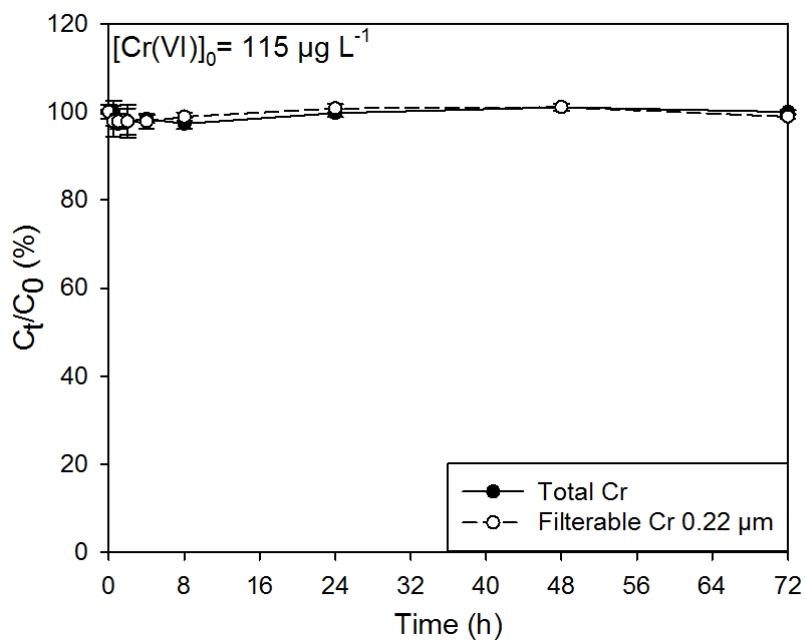
1033
 1034
 1035
 1036
 1037
 1038
 1039
 1040
 1041
 1042
 1043
 1044
 1045



1046
 1047 Figure S4. Temporal evolution (expressed as a percentage of the value measured at $t = 0$) of total Cr
 1048 concentrations in standard (ISO 8692) medium amended with initial concentrations of $\text{CrCl}_3 \cdot 6\text{H}_2\text{O}$
 1049 between 20 (C1) and 7000 (C9) $\mu\text{g/L}$ (see Table S2 for the full compilation of the measured values at t
 1050 $= 0$). Measurements were done in triplicate for C1, C2, C4 and C9 after 0 and 48 h of incubation. The
 1051 relative standard deviations (RSD) for these measurements were usually below 10 % except for C1 at
 1052 48 h (RSD = 20%) and C2 at 48 h (RSD = 15%).

1053
 1054
 1055 Table S2. Measured Cr concentration at $t = 0$ in standard (ISO 8692) medium amended with different
 1056 initial concentrations (C1–C9) of $\text{CrCl}_3 \cdot 6\text{H}_2\text{O}$ with and without filtration at $0.22 \mu\text{m}$. All values are in
 1057 $\mu\text{g/L}$ of Cr.

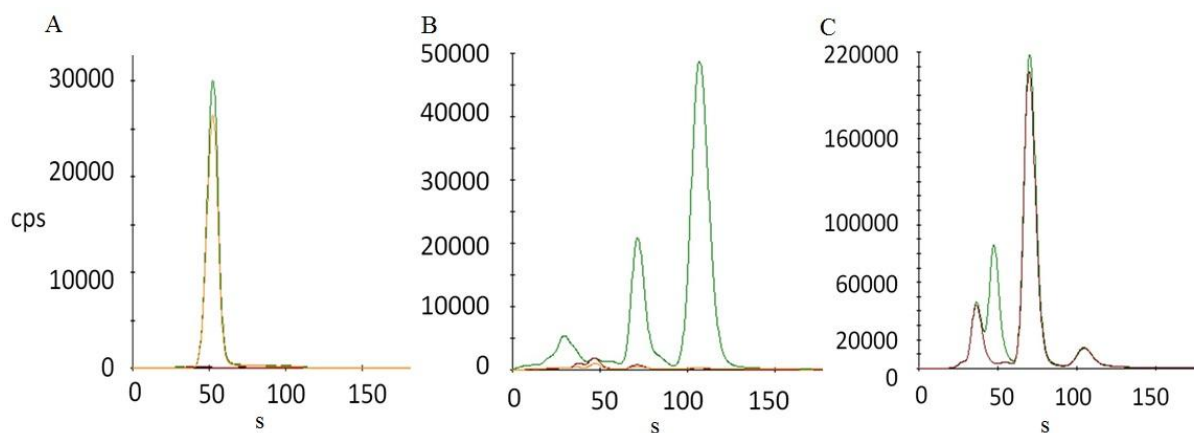
	Measured total concentration at $t = 0$	Measured filterable ($0.22 \mu\text{m}$) concentration at $t = 0$
C1	18	20
C2	40	42
C3	82	78
C4	186	179
C5	436	379
C6	789	717
C7	1745	1477
C8	3596	2700
C9	6877	5489



1059
 1060 Figure S5. Temporal evolution (expressed as a percentage of the values measured at $t = 0$) of Cr
 1061 concentrations (total Cr concentrations (black circles) and total dissolved Cr concentrations (filtered at
 1062 0.22 μm) (white circles) in biotic (presence of algae) ISO medium amended with Cr^{VI} ($\text{K}_2\text{Cr}_2\text{O}_7$)
 1063 during 72 hours. Initial Cr concentration is 115 $\mu\text{g/L}$.

1064
 1065
 1066
 1067
 1068
 1069
 1070
 1071
 1072
 1073
 1074
 1075
 1076
 1077
 1078
 1079
 1080
 1081
 1082

1083



1084

1085 Figure S6. Chromatograms of standard ISO 8692 biotic (presence of algae, initial density ~ 20,000
1086 cell/mL) medium amended with 115 $\mu\text{g/L}$ of Cr^{VI} ($\text{K}_2\text{Cr}_2\text{O}_7$) (A) or with 60 $\mu\text{g/L}$ of Cr^{III} ($\text{CrCl}_3 \cdot 6\text{H}_2\text{O}$)
1087 (B) at 0 h (green), 24 h (brown), 48 h (orange) or 72 h (blue) after spiking. Chromatograms of standard
1088 ISO 8692 medium containing 60 $\mu\text{g/L}$ of Cr^{III} ($\text{CrCl}_3 \cdot 6\text{H}_2\text{O}$) during 24 h (brown), and then amended
1089 with Cr^{VI} ($\text{K}_2\text{Cr}_2\text{O}_7$) (green) (C). All solutions were filtered (0.22 μm) immediately before analysis; cps
1090 (counts per second).

1091

1092

1093

1094

1095

1096

1097

1098

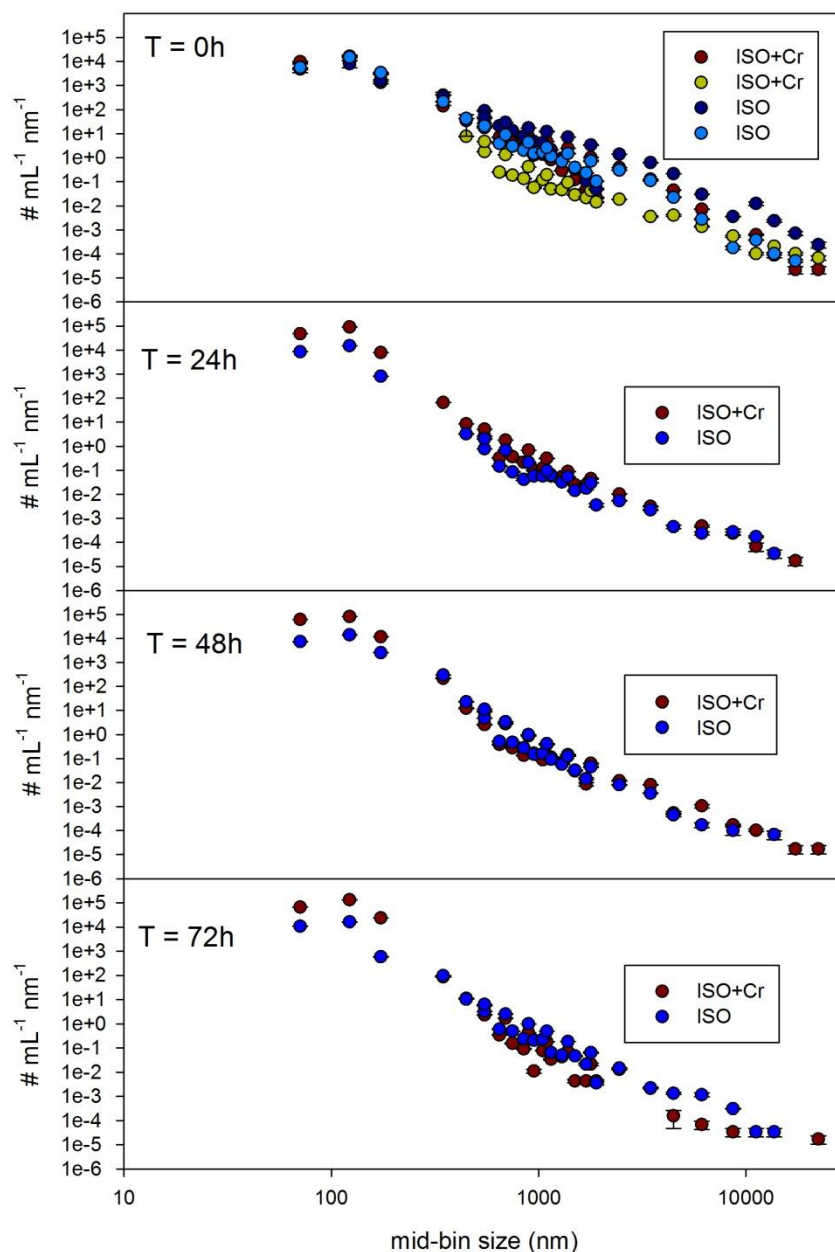
1099

1100

1101

1102

1103



1104

1105 Figure S7. Particle size distribution and number of particles (in mL⁻¹ nm⁻¹) determined with Single
 1106 Particle Counter (SPC) measurements in ISO algal test medium with and without addition of 70 µg/L
 1107 of Cr^{III} (added as CrCl₃.6H₂O) at different incubation times. To obtain the number of particles per mL
 1108 in a given size range, the values on the y-axis must be multiplied for the corresponding average size
 1109 value (in nm) on the x-axis.

1110

1111

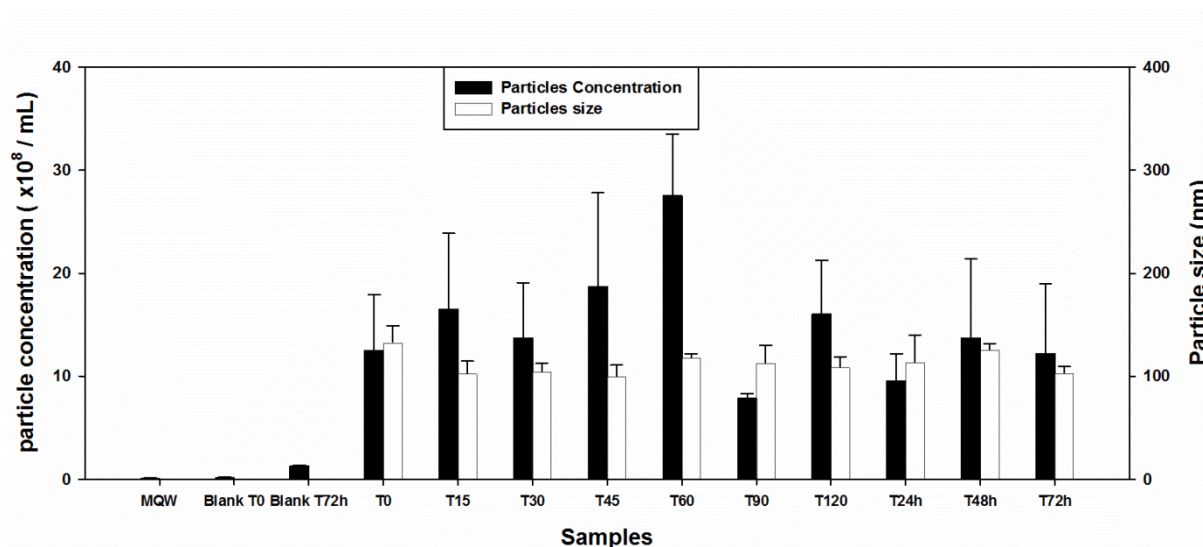
1112

1113 **Optimization of operating conditions for Nanoparticle Tracking Analysis with**
1114 **Nanosight NS500 instrument (Malvern instruments Ltd, UK)**

1115 In a preliminary experiment, aliquots of test medium spiked with 0, 17, 35, 70, 140 and 280
1116 $\mu\text{g/L}$, partly covering the concentration range used in toxicity test, were analyzed by NTA. No
1117 particles were observed in aliquots spiked with 17 $\mu\text{g/L}$ Cr^{III} and too many particles were
1118 detected in aliquots spiked with 140 $\mu\text{g/L}$ and 280 $\mu\text{g/L}$ Cr^{III} . Particle concentrations in the
1119 range $1\text{--}3 \times 10^9$ particles/mL were observed in solutions containing 35 and 70 $\mu\text{g/L}$ Cr^{III} . The
1120 latter concentration, closed to the observed 72h EC50 for Cr^{III} , was chosen for detailed
1121 analysis after 1, 15, 30, 45, 60, 90 and 120 min, and 24, 48 and 72 h of incubation.

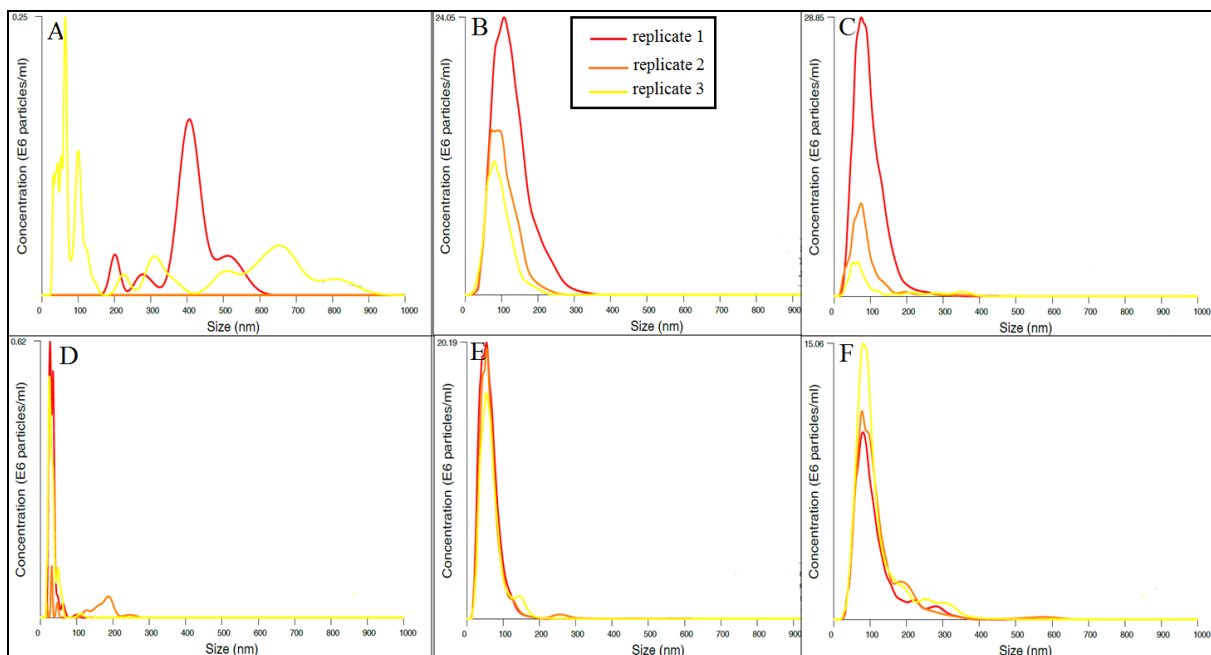
1122 No particles were detected in the ultrapure water (MQW) used to prepare the test medium.
1123 Particle concentration in the blank sample (freshly prepared ISO medium) was low ($0.14 \pm$
1124 0.07×10^8 particles/mL) and particle size distribution (PSD) covered a large spectrum
1125 between 0 and 900 nm (Figure S9). In ISO medium spiked with Cr^{III} and regardless of the
1126 incubation time, particle concentrations ranged between 7.85×10^8 and 27.5×10^8 particles/mL
1127 with relative standard deviations (RSD) between 6 and 59 % (Figure S8 and S9). Particles
1128 detected by NTA had a mean size between 100 and 135 nm with RSD between 1% and 12%
1129 (Figure S9). The high RSD of some particle concentration measurements were caused by the
1130 systematic decrease in particle number between the first and the third replicate measurement
1131 (Figure S9 A, B and C). The total (unfiltered) Cr concentration was stable over 72 h and
1132 ranged between 62 $\mu\text{g/L}$ at $t=0$ and 66 $\mu\text{g/L}$ 72 h after spiking. However, the total filterable Cr
1133 concentration decreased over time from 60 $\mu\text{g/L}$ at $t=0$ to 16 $\mu\text{g/L}$ after 72 h (Figure S10).
1134 Examination of the videos recorded during NTA showed that the number of particles visible
1135 in the field of the camera was stable during data acquisition for the first replicate, but
1136 increased with time for replicates two and three.

1137 Measurement parameters were modified by adding a waiting step of 60 s before data
1138 acquisition for replicates two and three and RSD on particle concentrations was reduced to 1–
1139 11% (Figure S9 D, E and F).



1140
1141 Figure S8. Particle concentration (black bars) and size (white bars) measured by nanoparticles tracking
1142 analysis (NTA) in standard (ISO 8692) medium spiked or not with 70 µg/L of CrCl₃·6H₂O for
1143 different incubation time between 0 and 120 min and after 24, 48 and 72 h.

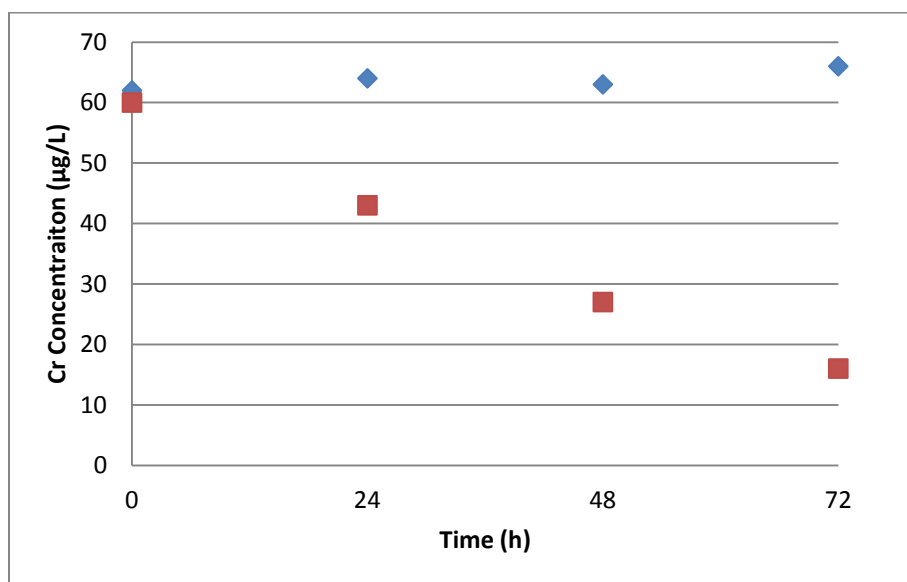
1144
1145
1146
1147
1148
1149
1150
1151
1152
1153



1154

1155 Figure S9. Comparison of reproducibility of results profiles before (A, B and C) and after (D, E and F)
 1156 measurement parameters modification by adding a waiting step of 60 s before data acquisition for
 1157 replicates 2 and 3. This edit to the experimental procedure aimed to harmonize the waiting time before
 1158 each replicate measurement; i.e. to increase the waiting time for replicates two and three from 5
 1159 seconds to 60 s. This experiment was realized in ISO test medium spiked with 60 $\mu\text{g/L}$ of Cr^{III} ,
 1160 corresponding to the previously determined EC50 at 72 h

1161



1162

1163 Figure S10. Temporal evolution of Cr concentrations in $\mu\text{g/L}$ (total Cr concentrations (blue squares),
 1164 and filterable Cr concentrations (0.22 μm) (red squares) in ISO medium amended with Cr^{III}
 1165 ($\text{CrCl}_3 \cdot 6\text{H}_2\text{O}$) during 72 hours. Initial nominal Cr concentration is 70 $\mu\text{g/L}$.

1166 **Corresponding spherical size and number concentration determination using single**
1167 **particle ICP-MS (spICP-MS) analysis using the Nexion 350 D**

1168 When nanoparticles arrive in the ICP-MS plasma they are turned into ions thus forming a
1169 cloud of ions. Truly dissolved ions are homogeneously distributed in solution and when
1170 injected into the plasma thus cause a continuous, yet fluctuating, stream of ions to be detected
1171 by the detector. Nanoparticles can thus be distinguished from dissolved ions as the former
1172 cause intensive peaks in the detected time dependent signal, each time a cloud of ions from a
1173 nanoparticle arrives at the detector. The intensity of this peak can be calculated into some
1174 measure of size, provided that a composition and shape are assumed for the particles (Table
1175 S3). Only one isotope (^{52}Cr) was measured simultaneously, whereas any Cr-containing
1176 particles formed because of hydrolysis most likely also contained oxygen atoms and protons.

1177 No collision cell gas was used to remove $^{40}\text{Ar}^{12}\text{C}$ interferences on the ^{52}Cr signal. Hence, a
1178 continuous background signal was recorded, not consisting of ^{52}Cr but of the $^{40}\text{Ar}^{12}\text{C}$
1179 interference. However, by using short dwell times, the intensity of any background signal
1180 reduces proportionally more than the short but intense nanoparticle signals [1]. It was thus
1181 hypothesized that better size detection limits could be obtained by using a relatively small
1182 dwell time, but still measuring in standard mode, where the sensitivity towards the most
1183 abundant Cr isotope (^{52}Cr) is highest. The used dwell time of 50 μs and the absence of settling
1184 time cause nanoparticle events to be spread over multiple subsequent measurement events that
1185 need to be integrated separately for each event. Moreover, distinguishing non-dissolved from
1186 dissolved signals was needed, because interferences still caused a relatively high background
1187 signal. Both requirements were achieved using a previously published method [2]. This
1188 method calculates an intensity cut-off value based on a number of times the standard
1189 deviation of the background signal. Integrated peak surfaces below this cut-off value are
1190 considered to stem from dissolved events and are not taken into account when recalculating

1191 the average signal and the standard deviation of the background signal. The method converges
1192 when no new particle events are identified and the particle size distribution is then calculated
1193 from the particle events intensities. Such a single cut-off value is known to lead to both false
1194 positives (peaks mistakenly considered particle events) and false negatives (peaks mistakenly
1195 considered dissolved events) [3]. The goal of the spICP-MS measurement was to verify the
1196 hypothesis of the presence of Cr-containing particles in the samples. Hence, a high and thus
1197 conservative number of standard deviations (5) was used to minimize false positives, rather
1198 than to minimize false negatives [4].

1199 The calculations were realized with a software called Nanocount, which is freely available at
1200 <http://blogg.slu.se/Nanocount>.

1201

1202

1203

1204

1205

1206

1207

1208

1209

1210

1211 Table S3: Conditions and ICP-MS parameters for spICP-MS analysis

ICP-MS parameters	
ICP-MS	Nexion 350D
nebulizer	GE Micromist
gas flow	0.87 L/min
plasma power	1,500 W
plasma gas flow	13.5 L/min
auxiliary gas flow	0.77 L/min
detector mode	pulse counting
KED	Standard
Data acquisition	
ions (m/z)	⁵² Cr
measurement unit	counts
sweeps/reading	10 ⁶
replicates	1
dwelt time	0.05 ms
integration time	50,000 ms
Data treatment	
Integration method	Fixed window
Peak integration time	20 ms
Minimum cluster size	4 ions
Signal discrimination method	Outlier analysis
Number of standard deviations for cut-off calculation	5
Assumed composition	Cr(OH) ₃
Assumed density	3.11 g cm ⁻³
Assumed shape	sphere

1212

1213

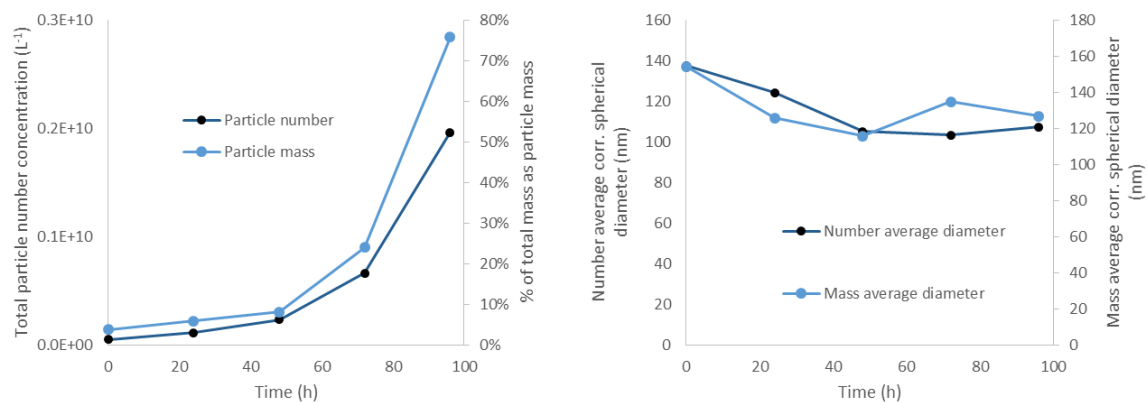
1214

1215

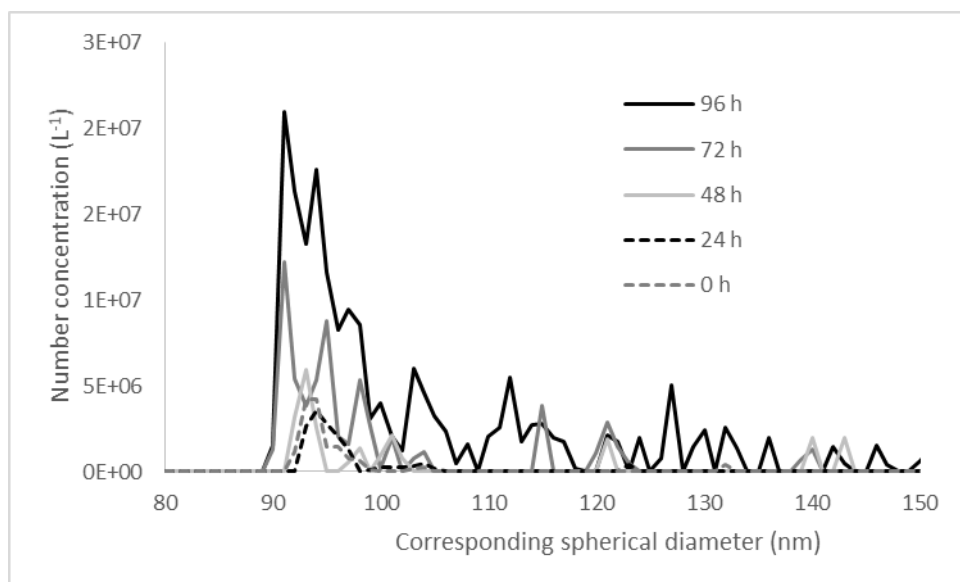
1216

1217

1218



1219
 1220 Figure S11. Temporal evolution of particle number and % of total mass occurring as particle mass
 1221 (left) or number average and mass average particle diameter (right). The diameters are corresponding
 1222 spherical diameters calculated using the setting in Table S3.
 1223



1224
 1225 Figure S12. Temporal evolution in the distribution of the corresponding spherical diameter. The
 1226 diameters are corresponding to spherical diameters calculated using the setting in Table S3.
 1227

1228
 1229
 1230
 1231
 1232
 1233

1234 **References**

1235 (1) Montaña MD, Badieli HR, Bazargan S, Ranville JF.2014. Improvements in the detection and
1236 characterization of engineered nanoparticles using spICP-MS with microsecond dwell times. *Environ.*
1237 *Sci. Nano.* 1(4): 338–346.

1238 (2) Tuoriniemi J, Cornelis G, Hassellöv MA.2015. new peak recognition algorithm for detection
1239 of ultra-small nano-particles by single particle ICP-MS using rapid time resolved data acquisition on a
1240 sector-field mass spectrometer. *J. Anal. At. Spectrom.* 30 (8): 1723–1729.

1241 (3) Cornelis G, Hassellöv MA.2013. signal deconvolution method to discriminate smaller
1242 nanoparticles in single particle ICP-MS. *J. Anal. At. Spectrom.* 29 (1): 134–144.

1243 (4) Tuoriniemi J, Cornelis G, Hassellöv M. 2012. Size Discrimination and Detection Capabilities
1244 of Single-Particle ICPMS for Environmental Analysis of Silver Nanoparticles. *Anal. Chem.* 84 (9):
1245 3965–3972.

1246

1247